SHALLOW SOIL MOISTURE - GROUND THAW INTERACTIONS AND CONTROLS

A Thesis Submitted to the
College of Graduate Studies and Research
in Partial Fulfillment of the Requirements
for the Degree of Master of Science
in the Department of Geography and Planning
(Centre for Hydrology)
University of Saskatchewan
Saskatoon, Canada

By

XIU JUAN (MAY) GUAN

PERMISSION TO USE

In presenting this thesis in partial fulfilment of the requirements for a Postgraduate degree from the University of Saskatchewan, I agree that the Libraries of this University may make it freely available for inspection. I further agree that permission for copying of this thesis in any manner, in whole or in part, for scholarly purposes may be granted by the professors who supervised my thesis work or, in their absence, by the Head of the Department or the Dean of the College in which my thesis work was done. It is understood that any copying or publication or use of this thesis or parts thereof for financial gain shall not be allowed without my written permission. It is also understood that due recognition shall be given to me and to the University of Saskatchewan in any scholarly use which may be made of any material in my thesis.

Requests for permission to copy or to make other use of material in this thesis in whole or part should be addressed to:

Head of the Department of Geography and Planning

University of Saskatchewan

Saskatoon, Saskatchewan

S7N 5C8 Canada

ACKNOWLEDGEMENTS

I would like to express gratitude and appreciation to my advisors Dr. Chris Spence and Dr. Cherie Westbrook for their insightful and supportive guidance. Chris and Cherie always made time to provide assistance and much appreciated advice. Thanks for their patience, faith in my abilities and for reiterating "think about your bumper sticker story" at the right times during writing. That did help. It has been a genuine pleasure to have worked with the two of them.

Thanks are also given to my advisory committee members for their constructive criticisms and helpful suggestions: Dr. John Pomeroy of the College of Arts and Science, Dr. Bing Si of the College of Agriculture and Bioresources and the School of Environment and Sustainability, Dr. Xulin Guo (Committee Chair) of the College of Arts and Science and Dr. Amin Elshorbagy (External Examiner) of the College of Engineering.

For field and/or logistical support, I would like to thank Ross Phillips of the Centre for Hydrology for his valuable assistance in the field and the canoe lessons. Newell Hedstrom of Environment Canada for his wonderful help with the field programs. The logistical support and hospitality extended to us in Yellowknife by Bob Reid of Indian and Northern Affairs Canada, the Water Survey of Canada staff (Northwest Territories and Nunavut branch), Dave Fox of Environment Canada, Corrie Mielko and Dane Gibson were much appreciated. More thanks to Mike Solohub for answering my equipment questions; Erin Shaw for agreeing to come winter camping with me; Dr. Julie Friddell of the Centre for Hydrology for her help with accounting logistics; as well as Dave and Rhonda Phillips for their kind help during camp wrap up.

I would also like to thank the students and staffs in the Department of Geography and Planning, particularly folks in the Centre for Hydrology for making the last few years highly enjoyable. A good support system was imperative for maintaining sanity in graduate school and I

was lucky to have a great group of peers including Adam, Erin C., Erin S., Jackie, Lawrence, Matt, Nathalie, Nicole, Ross and many other students. I am also very grateful to my family for their unconditional support and for bestowing upon me a good work ethic that proved indispensable for completing this degree.

Finally, I wish to thank the following organizations for funding this project: Environment Canada, International Polar Year, Canadian Foundation for Climate and Atmospheric Sciences via the Improved Processes and Parameterisation for Prediction in Cold Regions programme, Association of Canadian Universities for Northern Studies' Garfield Weston Award for Northern Research, and Indian and Northern Affairs Canada's Northern Scientific Training Program.

ABSTRACT

Soil moisture and ground thaw state are both indicative of a hillslope's ability to transfer water. In cold regions in particular, it is widely known that the wetness of surface soils and depth of ground thaw are important for runoff generation, but the diversity of interactions between surface soil moisture and ground thaw themselves has not been studied. To fill this knowledge gap, detailed shallow soil moisture and thaw depth surveys were conducted along systematic grids at the Baker Creek Basin, Northwest Territories. Multiple hillslopes were studied to determine how the interactions differed along a spectrum of topological, typological and topographic situations (T^3 template). Results did not show a simple relationship between soil moisture and ground thaw as was expected. Instead, correlation was a function of wetness such that the correlation between soil moisture and ground thaw improved with site wetness. To understand why differences in soil moisture and ground thaw state arose, water and energy fluxes were examined for these subarctic study sites to discern the key processes controlling the patterns observed. Results showed that the key control in variable soil moisture and frost table interactions among the sites was the presence of surface water. At the peatland and wetland sites, accumulated water in depressions and flow paths maintained soil moisture for a longer duration than at the hummock tops. These wet areas were often locations of deepest thaw depth due to the transfer of latent heat accompanying lateral surface runoff. Although the peatland and wetland sites had large inundation extents, modified Péclet numbers indicated that the relative influence of external and internal hydrological processes at each site were different. Continuous inflow from an upstream lake into the wetland site caused advective and conductive thermal energies to be of equal importance to ground thaw. The absence of continuous surface flow at the peatland and valley sites led to the dominance of conductive thermal energy over advective energy for

ground thaw. A quantitative explanation for the shallow soil moisture-ground thaw patterns was provided by linking hydrological processes and hillslope storage capacity with the calculated water and energy fluxes as well as the modified Péclet number. These results suggest that the T^3 template and the modified Péclet number could be very useful parameters for differentiating landscape components in modeling soil moisture and frost table heterogeneity in cold regions.

TABLE OF CONTENTS

LIST OF TABLES

LIST OF FIGURES

LIST OF SYMBOLS

a_b	Area of Bare Bedrock [m^2]
a_{bss}	Area of Bedrock Side Slopes [m^2]
A_c	Cross-Sectional Area [m^2]
a_s	Fraction of Area with Snow Cover [unitless]
a_{sc}	Area of Soil Covered Bedrock [m^2]
a_v	Area of Site [m^2]
C_{maxc}	Maximum Canopy Conductance [m d^{-1}]
C_{maxl}	Maximum Leaf Conductance [m d^{-1}]
c_p	Specific Heat of Moist Air [MJ kg^{-1} $ºC^{-1}$]
d	Snow Depth [m]
D	Vapour Pressure Deficit [kPa or mb]
dF/dt	Flow Rate [m^3 d^{-1}]
d_i	Rank Difference from *i*th Survey Grid
dT/dz	Temperature Gradient [ºC m^{-1}]
E	Evaporation [mm day^{-1}]
E_A	Mass Transfer [m d^{-1}]
ET	Evapotranspiration [mm day^{-1}]
f_a	Fraction of Air
f_i	Fraction of Ice
f_m	Fraction of Mineral Soil
f_o	Fraction of Organic Soil
f_s	Shelter Factor [unitless]
f(u)	Wind Function [mm k Pa^{-1} d^{-1}]
f_w	Fraction of Water
FT	Frost Table Depth [cm or m]
GEWEX	Global Energy and Water Cycle Experiment
GIS	Geographic Information System
h	Water Table Depth [m]
h_c	Height of Canopy Cover [m]
I	Inflow [mm day^{-1}]
I_{bss}	Runoff from Bedrock Side Slope over Study Site Area [mm]
I_s	Surface Inflow [mm day^{-1}]
I_{sb}	Subsurface Inflow [mm day^{-1}]
K	Saturated Hydraulic Conductivity [m s^{-1}]
K↓	Incoming Solar Radiation [W m^{-2}]
k_c	Unit Converter from MJ m^{-2} d^{-1} to mm d^{-1}
k_d	Diffusivity [m^2 s^{-1}]
K_T	Thermal Conductivity [W m^{-1} $ºC^{-1}$]
l	u_a Characteristic Length Scale [m]
Δl	Horizontal Distance Change [m]
LAI	Leaf Area Index [unitless]
LiDAR	Light Detection and Ranging
M	Melt [mm day^{-1}]

M_a	Ablation Rate [mm day^{-1}]
masl	Meters Above Sea Level
mPe	Modified Péclet number [unitless]
n	Number of Samples [unitless]
P	Precipitation [mm day^{-1}]
Pe	Péclet Number [unitless]
PET	Potential Evapotranspiration [mm day^{-1}]
Q	Discharge [mm day^{-1}]
Q*	Net Radiation [W m^{-2}]
Q_{fz}	Heat Released from Refreezing [MJ m^{-2} d^{-1}]
Q_g	Ground Heat Flux [MJ m^{-2} d^{-1}]
Q_{gf}	Total Ground Heat Flux into Frozen Ground [MJ m^{-2} d^{-1}]
Q_{gp}	Heat Conduction from Surface Water Ponding [MJ m^{-2} d^{-1}]
Q_{gs}	Heat Conduction from Surface Soil [MJ m^{-2} d^{-1}]
Q_{gw}	Heat Advection from Flowing Water [MJ m^{-2} d^{-1}]
Q_s	Surface Discharge [mm]
Q_{sb}	Subsurface Discharge [mm]
r_a	Aerodynamic Resistance [d m^{-1}]
R_b	Runoff from Bare Bedrock [mm]
R_{bss}	Runoff from Bedrock Side Slopes [mm]
r_c	Canopy Resistance [d m^{-1}]
r_{cmin}	Minimum Unstressed Canopy Resistance [d m^{-1}]
r_s	Spearman rank correlation coefficient [unitless]
R_{sc}	Runoff from Soil Covered Bedrock [mm]
RH	Relative Humidity [%]
s_b	Sublimation Loss [mm day^{-1}]
ΔS	Change in Storage [mm day^{-1}]
ΔS_o	Observed Change in Storage [mm day^{-1}]
ΔS_s	Saturated Storage Change [mm day^{-1}]
ΔS_u	Unsaturated Storage Change [mm day^{-1}]
SM	Soil Moisture [unitless or %]
SWE	Snow Water Equivalent [kg m^{-2}]
s_y	Specific Yield [unitless]
t	Time [day]
T	Temperature [ºC]
T^3	Topography, Topology and Typology
TDR	Time Domain Reflectometry
T_g	Soil Temperature [ºC]
t_o	Infiltration Opportunity Time [day]
U	Wind Speed [m s^{-1}]
u_2	Wind Speed at a Reference Height of 2 m [m s^{-1}]
u_a	Advection Rate [m s^{-1}]
u_{dir}	Wind Direction [degree]
u_m	Measured Wind Speed [m s^{-1}]
V_w	Volume of Water [m^3 m^{-2}]
z	Depth [m]

$\Delta \bar{z}$	Mean Snow Depletion [mm day^{-1}]
z_2	Desired Wind Speed at Reference Height of 2 m [m]
z_m	Actual Instrument Height [m]
z_w	Water Table Depth [mm]
γ	Psychrometric Constant [k Pa °C^{-1}]
Δ	Slope of Saturated Vapour Pressure [kPa °C^{-1}]
$\Delta\theta$	Daily Change in Soil Moisture Content [unitless]
λ_v	Latent Heat of Vapourization of Water [MJ kg^{-1}]
λ_f	Latent Heat of Fusion of Ice [MJ kg^{-1}]
ρ_a	Moist Air Density [kg m^{-3}]
ρ_s	Snow Density [kg m^{-3}]
ρ_w	Water Density [kg m^{-3}]

CHAPTER 1:

INTRODUCTION

Studies during the International Hydrological Decade (1965-1974) (e.g. Landals and Gill, 1972; Park, 1979) and the Mackenzie GEWEX Study (1993-2005) (e.g. Spence and Woo, 2006) provided many advances in the understanding of runoff generation in the subarctic Canadian Shield. Focus to date has been on the hydrological role of individual landscape elements in regulating water flow and storage. However, uncertainties remain on how soil filled areas regulate water flow and storage in northern regions. For instance, modeling of hydrograph responses in the lower Liard River valley, Northwest Territories has been unsuccessful due to the complex hydrological role of organic terrains in the area (Quinton et al., 2003). This complexity is in part caused by the presence of frozen ground that creates a unique dynamic boundary issue for subsurface water movement and storage. Lateral and vertical subsurface water fluxes are largely limited to the active layer, the zone above the permafrost that thaws annually during the spring and summer. Studies have started to link soil moisture with frost table dynamics, especially at wet locations (e.g. Carey and Woo, 2000; Hinkel and Nelson, 2003; Wright et al., 2009). However, detailed intra- and inter-site information is lacking in the literature. Since both soil moisture and frost table depth have important implications for water storage, greater certainty on their spatiotemporal link and their controls is needed to improve prediction of catchment storage and runoff in regions with frozen ground.

The goal of this thesis is thus to examine shallow soil moisture and frost table interactions in soil filled areas of the subarctic Canadian Shield. The next chapter will be a literature review of previous work on soil moisture and ground thaw patterns along with the importance of landscape structure. The research questions are also presented in Chapter 2. The study site is

described in Chapter 3 and all methods are described in Chapter 4. Chapter 5 examines the spatiotemporal link of soil moisture and frost table depth whereas Chapter 6 details the controls on these variables. Findings are synthesized in Chapter 7.

CHAPTER 2:

LITERATURE REVIEW

Reviewed in this section are soil moisture and ground thaw patterns, interactions and controls followed by the importance of landscape structure on these patterns.

2.1 Soil Moisture and Ground Thaw

Over 50% of Canada's land surface is underlain with discontinuous or continuous permafrost (Wolfe, 1998). A large portion of this area remains thoroughly frozen for at least six months each year and this duration increases with latitude. Water can flow in frozen soil, albeit slowly especially in ice rich soil (i.e. soil pores nearly or completely filled with ice). It is only in the spring and summer months when the mean air temperature remains above 0ºC can the frozen ground thaw - either entirely at locations with only seasonal frozen ground or partially at locations underlain by permafrost. Ground thaw has important implications on spatial and temporal soil storage capacities and runoff generation (e.g. Landals and Gill, 1972; Woo and Steer, 1983; Spence and Woo, 2003 and 2006; Wright et al., 2009). For instance, in peatland permafrost landscapes, hydraulic conductivity varies considerably over soil depth due to greater peat decomposition and humification with depth (Quinton and Marsh, 1998 and 1999). The water table depth in the peat partly controls the area contributing to runoff. The water table drops with ground thaw, which causes the contributing area to decrease due to an increase in subsurface storage capacity (Quinton and Marsh, 1999). Conversely, when the water table position is close to the surface, the source area increases with low flow resistance through the porous organic soils and along hollows (Quinton and Marsh, 1999).

Locations with the most thaw in the spring tend to remain as locations with the most thaw in the summer (Wright et al., 2009). Factors that cause localized differential ground thaw include

snow cover and vegetation cover. For example, radiated or advected melt energy from tree trunks can increase snow ablation in the immediate vicinity of the trunks at a faster rate than the surrounding (Faria and Pomeroy, 2000; Pomeroy et al., 2009); this exposes the soil earlier to direct solar energy and consequently, causes soils to thaw earlier. Patterns of earlier snow-free areas having deeper thaw depth are also noted by Shirazi et al. (2009). Lichen covered ground tends to have less thaw than mossy cover in the spring due to less efficient water retention properties; though this correlation weakens in the summer as the frost table and saturated zones deepen (Wright et al., 2009). Two key controls of frost table depth commonly mentioned in the literature are soil temperature and soil moisture (e.g. Gray et al., 1988; Kane et al., 2001; Wright et al., 2009). Wright et al. (2009) found wetter years tended to have deeper ground thaw at the inter-annual scale, but the seasonal correlation was not clear. Rouse et al. (1992) noted the opposite correlation at the seasonal scale; a dry season has more ground thaw due to more ground heat flux and thermal diffusivity.

Variable thawed depths have been shown to be strongly tied to spatial soil moisture distribution, especially in the spring when the deepest thaw was found at wetter locations (Wright et al., 2009). However, Woo and Xia (1996) studied the thermal condition of the active layer at a wetland site and at a drier site and found the wetland experienced less thaw than the drier site due to the ice content difference. Carey and Woo (1998a) had similar findings to Woo and Xia. They concluded ice rich locations increase the zero-curtain effect (i.e. latent heat keeps soil at isothermal (~0ºC) for long periods of time, Outcalt et al., 1990) and decreases the rate of ground thaw. A study in a continuous permafrost environment found soil moisture to be affected by: (1) intrinsic water retention and transmission properties of frozen and thawed soil; (2) the hydrological processes operating outside of the soil column, including precipitation and

meltwater runoff; and, (3) the thermal and hydrological processes occurring in the active layer that redistributes moisture (Woo and Marsh, 1990). While Woo and Marsh (1990) identified the hydrological processes that influence soil moisture in the active layer in continuous permafrost environments (Figure 2.1), their work was conducted only at the point scale.

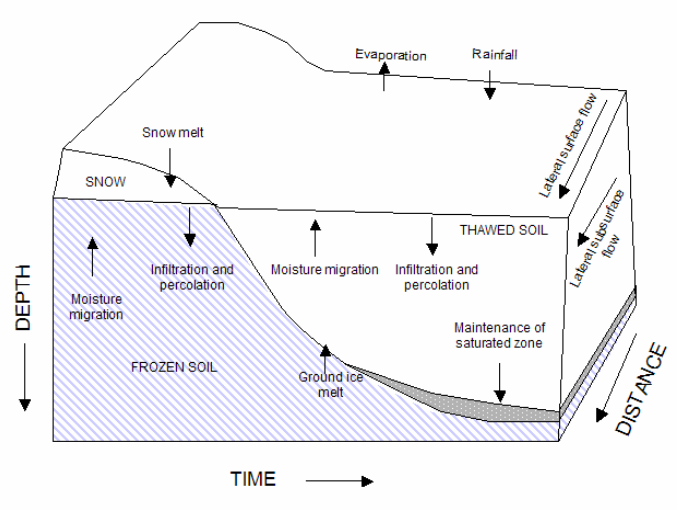

Figure 2.1 Conceptual framework showing the processes that affect soil moisture content in the active layer (Woo and Marsh, 1990).

Soil moisture has been the focus of many studies because of its control on hydrological processes through linking surface energy and water balances, vegetation growth and distribution (Grayson et al., 1997; Rodriguez-Iturbe et al., 2007). For long-term water balances, knowledge about the parts of the landscape that are wetter than the average can improve streamflow forecast models (Grayson et al., 1997). For example, Park (1979) found estimating soil moisture values for different land covers in the Baker Creek Basin yielded more accurate water balances than using one single, lumped value. Generally, soil moisture closer to the surface is more dynamic than at depth and can be a good indicator of surface runoff responses of soil (Western et al., 2002) and thus, shallow and deep soil moisture should be decoupled in models. For instance,

even small changes in the antecedent condition of surface soils can have dramatic non-linear changes in the runoff volume after a storm (James and Roulet, 2007). Spatial and temporal patterns of soil moisture are widely studied, most of which has been done in regions with a stable impermeable layer (i.e. bedrock). For instance, one of the most extensively studied catchments is at the Tarrawarra near Melbourne, Australia (e.g. Western et al., 2002; Grayson et al., 2002). Unlike other geographic regions, soils in cold regions are greatly influenced by ground thawing and freezing. Ice in frozen soil increases infiltrating water tortuosity and lowers the hydraulic conductivity and the rate of infiltration (Granger et al., 1984; Black and Miller, 1990).

A number of studies have alluded to linkages between ground thaw, soil moisture and surface water. Heat transfer from warmer surface water into the cooler soil has been found to have a strong influence on ground thaw in locations where there is convergence of lateral water flow into frost table depressions (Wright et al., 2009). Similarly, studies in the subarctic and the high arctic have found that surface water flow can enhance ground thaw on footslopes and preferential slope flow routes (Hastings et al., 1989; Hinzman et al., 1993; Carey and Woo, 1998b and 2000). At a subalpine slope in the Yukon Territory, ~9% of all incoming net radiation was directed to ground thaw in the spring (Shirazi et al., 2009) and there have been documented uses of more than 86% of the ground heat flux at a peat plateau used for melting the ground ice (Hayashi et al., 2007). Even though Carey and Woo (1998a) found no strong correlation between ground thaw and ground heat flux and suggested other factors have a more important influence on ground thaw, Hayashi et al. (2007) and Shirazi et al. (2009) noted differential thaw rates due to the thermal conductivity of peat, which is largely dependent on soil water content through its influence on thermal conduction.

Temperate region runoff generation patterns cannot simply be extrapolated to higher latitudes (Carey and Woo, 2001; Quinton and Carey, 2008). In areas with frozen ground, hydrological processes influenced by the frost table will need to be understood before patterns can be compared to those in temperate regions. As outlined above, both frost table topography and soil moisture strongly influence storage capacity (Spence and Woo, 2003; Wright et al., 2009). Further work to understand the relationship between soil moisture (in particular at shallow depth due to its nature as an indicative threshold) and ground thaw over different soil covers and understanding the controls on these patterns is needed to improve storage and runoff parameterization and prediction in cold regions.

2.2 Importance of Landscape Structure

A site's location in space can have an important influence on its hydrological behaviour. Landals and Gill (1972) found the timing of meltwater runoff differed among eight subarctic Canadian Shield sites with varied typology and topography. They noted that one of the key controls on the differences was topography because aspect and slope degree led to different ablation rates. In addition, relief difference and vegetation cover on sloped plots influenced snow distribution and runoff. In the same basin, estimating soil moisture values for different land covers (typology) helped yield more accurate water balances than using one single, lumped value (Park, 1979). Western et al. (2004) also found topography and soil properties to be important influences on soil moisture variation over space in a temperate rangeland site. Further, runoff generation in headwater subarctic Shield basins is also greatly influenced by topology (Spence, 2000).

Amongst the many factors that affect catchment hydrology, Buttle (2006) argues topography, topology (i.e. location in space, connectivity) and typology (e.g. soil, vegetation and

geology), referred to as T^3 template, are the three primary first order controls on streamflow response in catchments. He advocates a better understanding of catchment hydrology will be attained if these three controls are examined together rather than separately. As demonstrated above, each of the three traits have been studied and agreed upon to have strong influences on hydrological processes and fluxes in many landscapes. One advantage of using the T^3 template is that the findings encourage hydrologists to think about how the relative influence of each would change with scale (Buttle, 2006). For instance, under wet conditions when lateral processes dominate, drainage pathways and other spots with high water convergences are the wettest parts of a catchment and surface flow will first occur in these wetter areas when a large rain event occurs (Grayson et al, 1997). This response is through larger scale, nonlocal controls (Grayson et al., 1997). Under dry conditions when vertical processes dominate, soil moisture takes on more random patterns reflecting soil and vegetation heterogeneities (Grayson et al., 1997). At this time, only areas with local high convergence have organized soil moisture patterns and when a heavy rain event takes place, only areas where infiltration is exceeded will there be runoff (Grayson et al., 1997). With limited lateral flow and only local soil properties influencing spatial patterns, responses under dry conditions is through smaller scale, local controls (Grayson et al., 1997).

Comparably, it has been found water distribution in landscape units is correlated with landscape position or surface form (e.g. England and Holtan, 1969; Zebarth and De Jong, 1989). For instance, a strong correlation has been found between soil surface curvature and soil moisture (Sinai et al., 1981). To quantify variations that exist within a study site, Pennock et al. (1987) and Pennock (2003) developed a useful landform segmentation approach for the Saskatchewan Prairies.

These studies further establish that landscape location has an important control on soil water distribution. Not considered in the T^3 model, however was how soil moisture distribution can be heavily influenced by the presence of a soil column of variable thickness, as occurs in areas with permafrost. Further, many of the previous studies were reporting on the relationship between soil moisture and ground thaw only at the plot scale or on a single hillslope. Since the variance of topology, typology and topography over the watershed influences hydrological fluxes and responses, much more work is needed to discern the relationship between the dynamic thawing front and soil moisture patterns across a cold region landscape.

2.3 Research Questions

Hinkel and Nelson (2003) indicated the need to identify controls on small scale soil moisture and ground thaw patterns in order to discern the influences on larger scale runoff processes. The goal of this thesis is to improve understanding of the interrelations between spatiotemporal shallow soil moisture and ground thaw at common soil filled areas found across the discontinuous permafrost landscape of the subarctic Canadian Shield. The first set of questions asked in this thesis is:

1a. How do shallow soil moisture and frost table depth vary spatially and temporally?

1b. Is there a correlation between shallow soil moisture and frost table depth? If so, does the type of correlation vary with location?

As outlined above, recent studies have shown that the presence of soil water may enhance ground thaw. Understanding the hydrological and energy controls on this relationship are needed

to improve storage and runoff parameterization and prediction in cold regions. The second question asked in this thesis is thus:

2. What are the dominant hydrological and energy controls on the interaction between shallow soil moisture and frost table depth in soil filled areas located in the subarctic Shield?

CHAPTER 3:

STUDY SITE

Baker Creek Basin (62º35'N, 114º26'W) is a ~165 km^2 basin in the Northwest Territories, Canada located in the Taiga Shield ecozone that drains to Great Slave Lake (Figure 3.1). The basin is in the Slave Structural Province of the Canadian Precambrian Shield by the eastern boundary of the Interior Plain (Wolfe, 1998). When the area was inundated by glacial Lake McConnell during the Wisconsin glaciation, lacustrine materials were deposited in local depressions (Park, 1979; Wolfe, 1998). Many areas in the basin are usually isolated and only spill and drain to Baker Creek in the wettest periods (Park, 1979). The West Bay fault greatly influences Baker Creek's drainage pattern by creating a linked flow pattern in the southeasterly direction (Wight, 1973; Park, 1979). The area is underlain by discontinuous permafrost which is typically found under organic-rich soil (Wolfe, 1998). It is at the widespread (50% to 90%) to sporadic (10% to 50%) permafrost boundary (Wolfe, 1998). Spence (2006) noted that when the A horizon is comprised of glacial lacustrine clays, permafrost is usually present.

The basin has a continental subarctic climate and air masses predominantly originate in the Arctic Ocean during winter and spring and in the Pacific Ocean during summer and fall (Wolfe, 1998). Climate normals from 1971-2000 at Environment Canada's climate station, Yellowknife A (62º27'N 114º26'W) show a mean annual temperature of -4.6ºC, a January mean of -26.8ºC and a July mean of 16.8ºC. The annual precipitation is 281 mm with 59% falling as rain. In the summer months, a high evaporation to precipitation ratio is common, and this often results in a negative water balance within the isolated soil filled areas before fall freeze-up (Spence and Rouse, 2002). The basin's mean annual runoff ratio is 0.21 (Spence et al., 2009). Some of the key factors controlling the basin's storage capacity and infiltration rates are the Shield's

extensive bedrock outcrops, short snowmelt duration, and presence of frozen ground (Landals and Gill, 1972). Park (1979) noted that in areas where isolated local depressions exist, a large volume of annual runoff can be retained. Soil filled areas occupy 44% of Baker Creek Basin – with 19% open black spruce forest and 25% peatland. The remaining dominant land covers are exposed bedrock (30%) and surface water (19%) (Spence et al., 2009). Three soil filled areas (a peatland site, a valley site and a wetland site) representative of the range of topographic, topological and typological of soil filled areas in the basin were chosen for intensive study (Figure 3.2 and Table 3.1).

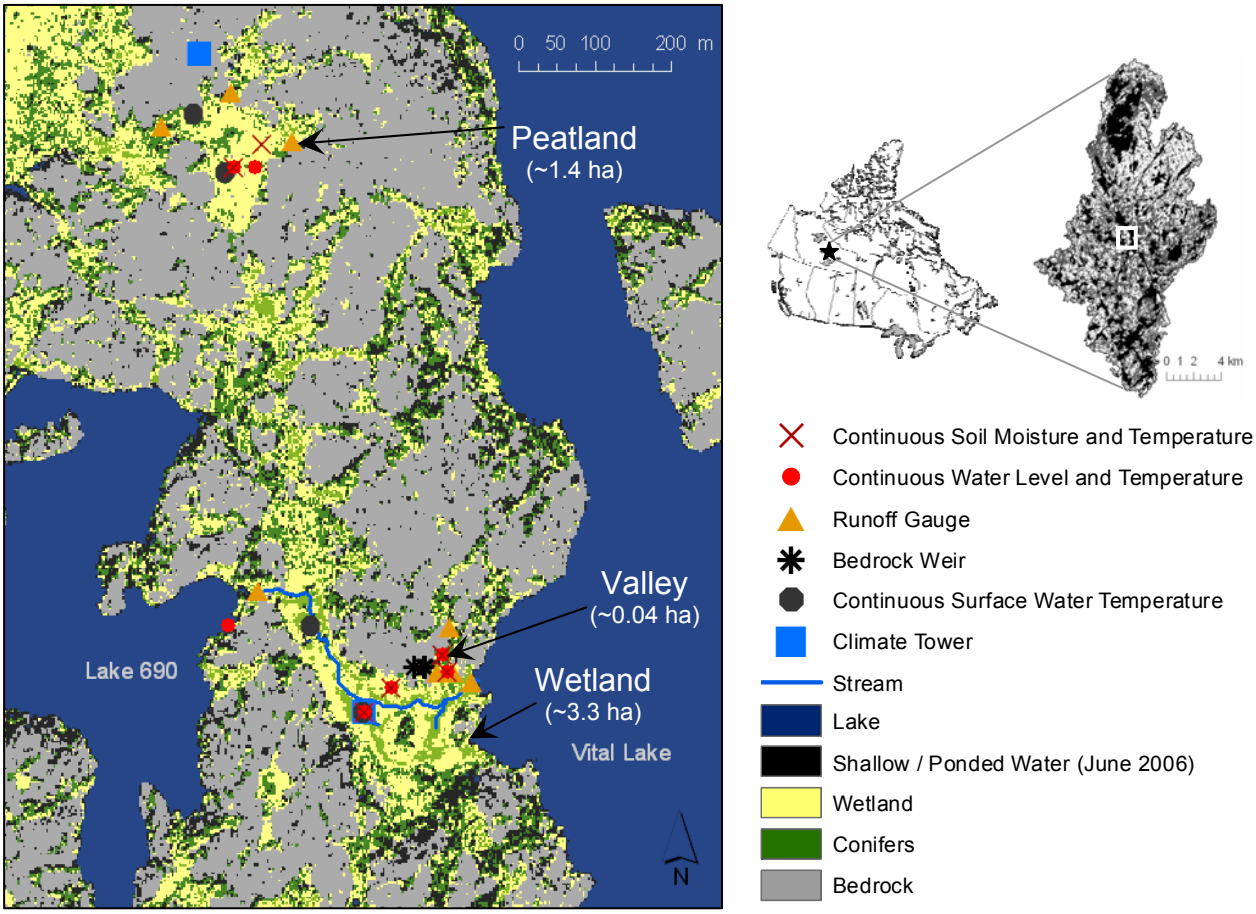

Figure 3.1: Instrument locations, land cover classification (left, June 2006 Quickbird satellite imagery, 2.5 m resolution) and total survey area of the three study sites. The insets show the ~165 km^2 Baker Creek Basin (right, Landsat imagery) with the solid black indicating location of lakes.

Figure 3.2: The selected study sites: (a) peatland site, with a piezometer nest in foreground, (b) valley site, facing upslope, north-northeast, and (c) wetland site with Vital Lake in background. Arrow shows location of climate tower.

Table 3.1: Site area, topographic gradient based on 1 m by 1 m digital elevation model, size of the survey grids, total number of shallow soil moisture and frost table sample points (n), shallow soil characteristics (top 0.10 m), and saturated hydraulic conductivity (K) at each site. Shallow and deep K are at pipe slot depths described in section 4.5.4.

Site	Peatland	Valley	Wetland
Area (ha)	1.4	0.04	3.3
Gradient (%)	3	12	6
Survey Cell Size (m)	4 x 8	2 x 2	15 x 15
n	358 – 380	81 - 91	102 – 117
Soil Porosity	0.85	0.83	0.80
Soil Bulk Density (kg m^{-3})	78	113	104
Soil Particle Density (kg m^{-3})	574	644	567
Soil Specific Yield	0.15	0.19	0.25
$K_{shallow}$ (m s^{-1})	10^{-6}	10^{-5} to 10^{-7}	10^{-6} to 10^{-7}
K_{deep} (m s^{-1})	10^{-7} to 10^{-8}	10^{-8} to 10^{-9}	10^{-6} to 10^{-9}

3.1 Peatland Site

Vegetation at the peatland site (Figure 3.2a) is approximately half nonvascular plants (dominated by lichens) and half vascular plants (dominated by evergreen shrubs). Vegetation includes Labrador tea (*Ledum groenladicum*), leatherleaf (*Chamaedaphne calyculata*), dwarf bog rosemary (*Andromeda prolifera*), lichen (*Cladina* spp. and *Cladonia* spp.), *Sphagnum* spp., northern bog laurel (*Kalmia polifolia*), cloudberry (*Rubus chaemorus*), and sparse stands of black

spruce (*Picea mariana*) and Jack pine (*Pinus banksiana*). Plant nomenclature follows Johnson et al. (1995). The overall average vascular plant height is ~0.3 m.

The peatland site has ~1.2 m of peat overlying the bedrock. Table 3.1 lists the laboratory results of soil porosity, bulk density, particle density and specific yield (s_y) tests of the top 0.10 m of soil at each site and Figure 3.3a shows the shallow soil. Saturated hydraulic conductivity (K) was measured in the piezometers installed at each site and calculated with the Luthin approach (1966), a common method used in the arctic (e.g. Woo and DiCenzo, 1989; Quinton et al., 2000; Hodgson and Young, 2001). Shallow hydraulic conductivity is listed in Table 3.1. There is increasingly packed peat with depth and this is reflected by the lower K at depth (Table 3.1).

The site is hydrologically isolated because it is surrounded by bedrock. It has a number of soil filled bedrock inlets to the east. There are two outlets, the key outlet is at the northwest section of the site through a wide, moss and treed covered area. The inlets and outlets flow during snowmelt and after heavy rains.

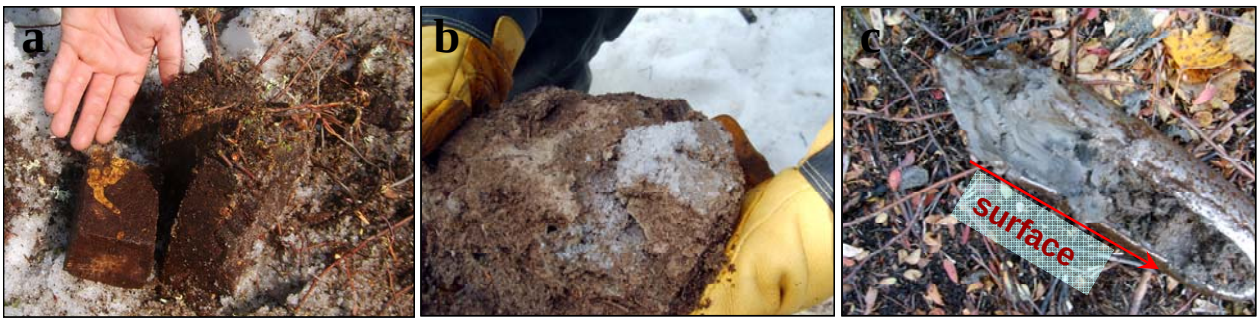

Figure 3.3: Shallow soil at: (a) peatland site, (b) valley site, and (c) wetland site.

3.2 Valley Site

The valley site is treed with bedrock on two sides and drains into the studied wetland site. It is dominated by arboreal vegetation (Figure 3.2b) such as black spruce. Other plant species at the

site include green alder (*Alnus crispa)*, willow (*Salix* spp.), birch (*Betula* spp.), prickly rose (*Rosa acicularis*), dwarf bilberry (*Vaccinium caespitosum*), lichen (*Cladina* spp. and *Cladonia* spp.), and *Sphagnum* spp. The site's overall average vegetation height is ~7 m.

The valley site has a thin organic layer (mean of 0.20 m) which overlies loose gravels, silty clay and sandy clay (Figure 3.3b). The site slopes south-southwest towards the wetland site. In addition to runoff from bare bedrock, the site has a defined soil filled bedrock inlet. There are two water eroded outlets toward the bottom of the site with one channel on each side adjacent to the bedrock slopes. Similar to the peatland site, the valley inlets and outlets are only active during snowmelt and following larger rain inputs. The slope of the peatland site and wetland site is low whereas the valley site is steeper (Table 3.1).

3.3 Wetland Site

The site is situated between two lakes, Lake 690 (unofficial name) and Vital Lake. Water drains from Lake 690, flows through the wetland site (in well defined channels in some areas) and then empties into Vital Lake (Figure 3.2c). During the 2008 field season, there was continuous inflow and outflow. The site is hummocky with many waterlogged hummock depressions that remain permanently wet in the thaw seasons. The peatland site is more hummocky but less waterlogged than the wetland site as the main source of water is from snowmelt runoff versus the wetland sources that include meltwater runoff and continuous input from Lake 690.

Deciduous shrubs dominate the vegetation cover at the wetland site (4.2c). Vegetation includes willow (*Salix* spp.), green alder (*Alnus crispa)*, birch (*Betula* spp.), leatherleaf (*Chamaedaphne calyculata*), small bog cranberry (*Oxycoccus microcarpus*), *Sphagnum* spp., and

shrubby cinquefoil (*Potentilla fruticosa*). Stands of black spruce and birch occur on raised ground and tamarack is found at the southwest portion of the site. Longlasting ponded areas below the Lake 690 outlet support other aquatic plants including swamp horsetail (*Equisetum fluviatile*), water arum (*Calla palustris*), sedge (*Carex* sp.) and marsh cinquefoil (*Potentilla palustris*). The average height of vegetation at the site is ~1.4 m.

The wetland site has 0.20 m to 0.60 m of peat over impervious lacustrine clay (Figure 3.3c). There was a wide range of K in the deeper soils due to variation in the presence of peat and clay (Table 3.1).

CHAPTER 4:

METHODS

4.1 Study Design

Field work was conducted between 14 April and 17 July 2008. Elevation, shallow soil moisture and frost table surveys were measured in systematic grids. The grid cell size (Table 3.1) was based on total site area and feasibility to complete each site survey on the same day. The grids were set up as soon as the ground was near snowfree. Sample points were marked using various combinations of a survey level, stadia rod, survey tape and compass. The points were flagged to keep the measurement locations constant. The resolution of surveys and the total number of points are listed in Table 3.1. The coordinates and elevations at each of the survey grids were surveyed using a Sokkia SET610 total station with a CST 63-2010M prism and referenced to meters above sea level (masl). At each site, a flat reference location for the tripod on the bedrock was chosen, and the global positioning system coordinates of the location was used to find the elevation for the point from a 1 m by 1 m digital elevation model layer from a Light Detection and Ranging (LiDAR) survey (Hopkinson and Fox, 2008). All subsequent locations from each site were then surveyed relative to the initial tripod location.

4.2 Shallow Soil Moisture

To measure shallow soil moisture (i.e. top 0.10 m), two portable time domain reflectometry (TDR) units were used, the first unit was with a Campbell Scientific TDR100 wired to a CR10X datalogger; this TDR probe was built in the laboratory at the University of Saskatchewan. The second unit also had a TDR100 but was wired to a CR800 with a CS640 TDR probe. Surveys were completed at average every two days in May and then less frequent in June and July. Site

specific gravimetric soil samples were extracted and used to calibrate both units in the laboratory. Three samples from each of the three study sites were used for the test. The samples were wetted and dried in a soil oven over time increments and subsequently calibrated against gravimetric estimated soil moisture. A total of 51 points for the peatland site, 50 points for the valley site and 51 points for the wetland site were used to calibrate the unit with the CR800. An additional 54 points were used to standardize the CR10X unit against the CR800 unit. The calibration curves are in Appendix A. Saturated points were recorded as the site's maximum volumetric water content (i.e. soil moisture) determined by total void space listed as total soil porosity in Table 3.1. In the rest of the thesis, soil moisture will be referring to shallow (0.10 m) soil moisture, unless stated otherwise. At locations with surface ponding, depth of ponding was also recorded.

4.3 Frost Table

In each grid, the depth to the thawing front (i.e. frost table) was measured by pushing a steel rod into the thawed soil until denial. Maximum recordable depth was 1 m. Table 3.1 lists the total number of surveyed points for each survey date. When seasonal frozen ground was thawed, the point was removed from the dataset used to analyze the interaction between shallow soil moisture and frozen ground.

4.4 Spatiotemporal Soil Moisture and Frost Table Depth Maps

Site boundaries were mapped using the survey extent and a classified Quickbird satellite image (Figure 3.1) as guides. Surface ponding, shallow soil moisture and frost table spatial patterns on each sample date were mapped in ArcGIS 9.3. Cell resolution was set to equal the field measurement resolutions at the valley and wetland sites. At the peatland site, the field

survey was not completed in a square grid and thus the GIS (Geographic Information System) cells were set to 8 m x 8 m.

4.5 Water Fluxes

At each site, the water fluxes shown in the water budget (Equation 1) were measured or calculated to elucidate the measured soil moisture and frost table patterns:

$$P + M + I - Q - ET = \Delta S \qquad (1)$$

where P is precipitation, M is melt, I is inflow, Q is discharge, ET is evapotranspiration, and ΔS is change in storage (all units are mm d^{-1}). The difference between calculated ΔS and observed storage change (ΔS_o) was used to calculate a missing flux, when necessary.

4.5.1 Meteorological Measurements

Meteorological data were collected on the bedrock above the peatland site and in the wetland site (Figure 3.1). The peatland station was installed on bare bedrock with sparse tree cover and the wetland station was at a partly saturated area with deciduous shrubs in its immediate surrounding. The peatland station measured air temperature, T (ºC) and relative humidity, RH (%) at two heights, wind speed, u (m s^{-1}), wind direction, u_{dir} (degree), net radiation, Q* (W m^{-2}), and rainfall, P (mm). The instruments were connected to a Campbell Scientific CR23X datalogger. T and RH at two heights, u, Q* and P were also measured at the wetland site with a Campbell Scientific CR1000 datalogger. Data were scanned every minute and averaged at half-hour intervals.

4.5.2 Snow Survey and Snow Cover Interpolation

Snow surveys were completed at each of the three study sites following the methods described in Pomeroy and Gray (1995) and Woo (1997) (accuracy within 15%). Surveys were completed along transects at ~5 m intervals, and at every fifth depth measurement, a density sample was taken. Snow depth was measured with a metal meter stick and snow density samples were taken with an Eastern Snow Conference snow sampler. Mean snow water equivalent, SWE (mm) was calculated for each transect using:

$$SWE = \frac{\rho_S d}{\rho_W} \qquad (2)$$

where ρ_s is snow density (kg m^{-3}), d is mean snow depth (mm) and ρ_w (1000 kg m^{-3}) is water density. All individual SWE samples were averaged over site to obtain an overall mean SWE for each site. After the snow survey, to account for any newly fallen snow, one snowboard was set up by each ablation line (section 4.5.3) and monitored daily.

4.5.3 Melt

An ablation line was set up at each of the three sites to monitor daily ablation rate (M_a) following the approaches described in Heron and Woo (1978) (accuracy within 25%). Each line consisted of 10 points, and at the time height to snow measurements were made, surface (top 16 mm) snow density samples were also collected. The daily depth of melt rate (M, mm day^{-1}) at each soil filled zone was calculated as**:**

$$M = \left(\underbrace{(\Delta\bar{z})\frac{\rho_s}{\rho_w}}_{M_a} - s_b \right) a_s \qquad (3)$$

where $\Delta \bar{z}$ is mean snow depletion between two consecutive days (mm day^{-1}) and s_b is sublimation loss (mm day^{-1}). The s_b was calculated with the latent heat available for vapourization using latent heat flux data from the peatland climate station. The rates were weighted to the fraction of area with snow cover (a_s, unitless) at each of the sites estimated from daily site photos.

4.5.4 Inflow

Surface inflow (I_s) stations that were channelized were measured with a SonTek FlowTracker acoustic doppler velocimeter. Channelized inflow into the peatland site was measured every one to two days from two bedrock runoff stations, and at the valley and wetland sites, from one station at each site (Figure 4.1). The inflow to the wetland site from Lake 690 was a thoroughly documented location during the study period. A Solinst Levelogger was placed in Lake 690 to monitor the lake stage every half-hour. These data were used to find a stage-discharge relationship at the inlet (Appendix B). The lake water level was also manually measured with a survey level at approximately once a week during the study period and opportunistically at other times to adjust the Levelogger readings if necessary. Half-hourly readings from a Solinst Barologger installed at the wetland site were used to compensate Levelogger readings for fluctuations in barometric pressure.

Field data were used to model flow from soil covered and bare bedrock into the sites. For bedrock with soil cover, data from the two peatland inlets and one valley inlet were used. Values were sometimes overestimated since measurements were done only when there was enough water to fully submerge the velocimeter. For bare bedrock upland runoff, sheet metal weirs comparable to those used by Spence and Woo (2002) (Figure 4.1b) were installed in fall 2007. The recorded runoff volumes were converted into depths based on the bedrock contributing area

to the weirs. The boundaries of the contribution area were visually delineated in the summer based on best judgment and then surveyed with the total station. To calculate total lateral inflow from the surrounding bedrock upland (both bare and soil covered bedrock), the contribution areas to each site were delineated with the watershed tool in the ArcGIS hydrology spatial analyst toolbox using data from a 1 m resolution digital elevation model. After the total contribution area was delineated, the Quickbird satellite image and observations were used to categorize all bedrock side slopes as either bare or soil covered to model flow from each category separately. To prevent bare bedrock that flows into soil covered bedrock from being accounted twice (i.e. once as bare bedrock runoff and then again for soil covered bedrock), all bare areas contributing to soil covered bedrock were subtracted from bare bedrock runoff calculations. Runoff from the bedrock side slopes (R_{bss}) was calculated as:

$$R_{bss} = \frac{(R_b a_b) + (R_{sc} a_{sc})}{a_{bss}} \qquad (4)$$

where R is runoff generated (mm), a is area (m^2) over which runoff is generated, subscripts bss, b, and sc are bedrock side slope, bare bedrock and soil covered bedrock, respectively. To convert R_{bss} from depth of runoff per unit area of bedrock side slope into depth over each of the study sites (I_{bss}), the following equation was used:

$$I_{bss} = \frac{R_{bss} a_{bss}}{a_v} \qquad (5)$$

where a_v is the site area. At sites where lake inflow was measured (e.g. the wetland site), I_{bss} was added to it to get total I_s into the soil filled site.

Fully slotted wells in the form of rigid polyvinyl chloride pipes capped at the bottom were installed to monitor the suprapermafrost groundwater storage. Piezometer nests were installed at

each site to monitor vertical water flux. At the peatland site, there were three wells, and five piezometer nests with slots at depths (A) 0.20 m and (B) 0.50 m. The valley site had four wells and five piezometer nests with two out of the five with a C pipe as well. The slot depths were variable for the site due to loose rocks in the substrate that made installation of pipes to a constant depth difficult. The A slots were all ~0.20 m, the B slots averaged ~0.35 m and the two C slots were 0.50 m and 0.55 m. Five wells and eleven piezometers nests at slot depths of 0.20 m and 0.50 m were monitored at the wetland site. Three additional piezometers were installed along the stream. The hydraulic heads in the piezometers installed in the streambed were compared with stream hydraulic heads to determine if the stream was losing or gaining water. Subsurface inflow was only estimated at the wetland site. At the valley site, the combination of frozen soil around the slots, water table depth being deeper than the thawed slotted depths and dried locations did not provide enough information to calculate subsurface flow over the study period. Due to the peatland site's extensive bedrock surrounding, no subsurface inflow was measured at the site and the installed pipes were not able to capture the flow properties toward its northwest outlet. At the wetland site, I_{sb} was calculated as:

$$I_{sb} = \frac{K(h_1 - h_2)}{\Delta l} A_c \qquad (6)$$

where I_{sb} is subsurface inflow (mm), K is hydraulic conductivity (m d^{-1}), $(h_1-h_2)/\Delta l$ is hydraulic gradient with water table level difference (h_1 and h_2) over distance between the piezometer nests installed in a soil filled valley upslope of the wetland (Δl) (m m^{-1}) and A_c is cross-sectional area (m^2). I_{sb} was then converted to depth (mm) by dividing the total site area.

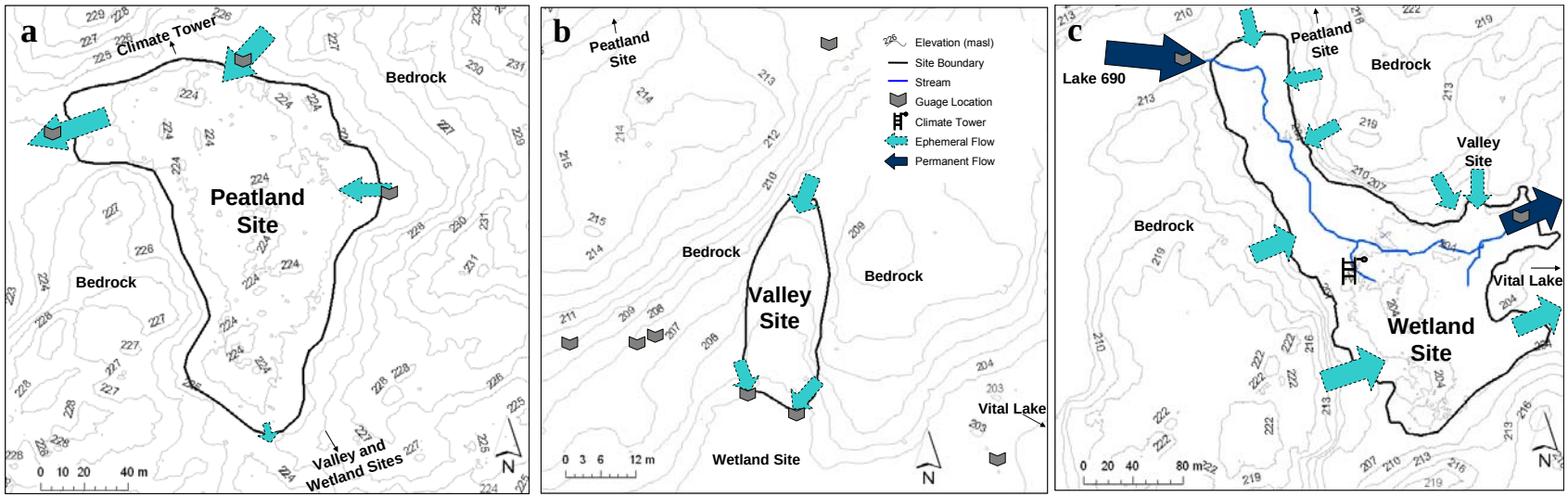

Figure 4.1: Main surface flow lines and elevation map of the study sites. The contour interval at the peatland site (a) is 1 m, 1 m at the valley site (b) and 3 m at the wetland site (c). Elevations are referenced to masl. Size of arrows is proportional to flow magnitude (e.g. larger arrow indicates relatively greater water flow).

4.5.5 Discharge

The surface discharge (Q_s) from the peatland site was measured at its main outlet at the northwest end of the site (Figure 4.1a). However, due to the outlet's extensive moss cover with alternating subsurface to surface flow, the measured values did not always capture the full extent of outflow from the site during snowmelt. Thus, the residual of the water budget storage was computed to more accurately estimate discharge on days with missing or suspect data. Outflow from the valley was gauged at two locations. At the foot of the site, there was an eroded soil channel at the base of both bedrock slopes and outflow was gauged during snowmelt (Figure 4.1b). One location was gauged at the wetland site (Figure 4.1c). Only Q_s flow through the wetland outlet was continuous during the study. With widespread sheetflow until mid-June when lower flows finally became channelized, outflow at this location was also not measurable, and similar to the peatland outlet, flow from those dates were calculated with the residual of the water budget. The subsurface outflow, Q_{sb} was measured with the same approaches as described for I_{sb} in section 4.5.4.

4.5.6 Evapotranspiration

Evapotranspiration (ET) was calculated using the Penman-Monteith equation as described in Shuttleworth (1993):

$$ET = \frac{1}{\lambda_v}\left(\frac{\Delta(Q^* - Q_g) + \dfrac{\rho_a c_p D}{r_a}}{\Delta + \gamma\left(1 + \dfrac{r_c}{r_a}\right)}\right) \qquad (7)$$

where λ_v is latent heat of vapourization of water (MJ kg^{-1}), Δ is slope of saturated vapour pressure (kPa $°C^{-1}$), Q* is net radiation (MJ m^{-2} d^{-1}) measured at the wetland site with a Kipp & Zonen

NR-LITE net radiometer, Q_g is ground heat flux (MJ m^{-2} d^{-1}), ρ_a is moist air density (kg m^{-3}) calculated with the ideal gas law, c_p is specific heat of moist air (0.001013 MJ kg^{-1} $^oC^{-1}$), D is vapour pressure deficit (kPa), r_a is aerodynamic resistance (d m^{-1}), γ is psychrometric constant (k Pa $°C^{-1}$), and r_c is canopy resistance (d m^{-1}). The Q_g was calculated with the Fourier heat flow equation:

$$Q_g = K_T \frac{T_{g2} - T_{g1}}{z_2 - z_1} \qquad (8)$$

where T_g is soil temperature (ºC) measured with ECH$_2$O-TE sensors connected to Em50 analogue dataloggers at each of the sites at two depths (z) (i.e. just below surface and 0.25 m below ground surface). Data were recorded every half hour and then averaged daily. Thermal conductivity, K_T (W m^{-1} $^oC^{-1}$) was calculated as the function of the fraction of mineral soil (f_m), organic soil (f_o), ice (f_i), water (f_w) and air (f_a) multiplied by each medium's thermal conductivity (de Vries, 1963; Farouki, 1981):

$$K_T = (2.93^{f_m})(0.25^{f_o})(2.20^{f_i})(0.57^{f_w})(0.025^{f_a}) \qquad (9)$$

The fractions of mineral and organic soils are constant over time and they were based on soil pit observations and soil sampling taken for soil moisture sensor calibrations. Initial ice content was determined by the antecedent soil moisture conditions measured with a calibrated Theta Probe (type ML2x) at the valley site, and with the ECH$_2$O-TE sensors at the peatland site in September 2007. However, moisture migration overwinter has been documented in literaute (Woo and Marsh, 1990). The wetland area below the inlet was ice covered at the beginning of the study period indicating a saturated antecedent soil moisture condition. In early spring, when thaw

depth was less than 0.25 m from ground surface, the daily fractions of ice and water were interpolated from measured frost table positions. The fraction of air was calculated as the residual of porosity minus ice and water fractions. Q_g was then converted from W m^{-2} to MJ m^{-2} d^{-1}.

The r_c was calculated with a revised version of the Jarvis (1976) and Verserghy et al. (1993) expression (Lafleur and Schreader, 1994) using environmental conductance functions of incoming solar radiation, K↓ (W m^{-2}), and D (mb):

$$r_c = r_{c\min} f(K\downarrow) f(D) \qquad (10)$$

where r_{cmin} is minimum unstressed canopy resistance (d m^{-1}). The vegetation cover at the peatland site is approximately half nonvascular plants and half vascular plants. The r_{cmin} of lichen used for the calculations is 0.00016 d m^{-1}, the value from studies of *Cetraria nivalis* clumps (Larson and Kershaw, 1976). Limited r_{cmin} data are available for natural vascular plants, however, its inverse, maximum canopy conductance, C_{maxc} (m d^{-1}) has been better studied. C_{maxc} was calculated with the method described in Dingman (2008):

$$C_{\max c} = f_s \, LAI \, C_{\max l} \qquad (11)$$

where f_s is shelter factor that ranges from 0.5 (fully vegetated) to 1.0 (sparsely vegetated) (Carlson, 1991). The f_s at all locations except for the vascular plant cover at the peatland site were set as 0.5, which is a good approximation of a fully vegetated area (Allen et al., 1989). The vascular plant cover at the peatland site was set at 0.8 due to more sparsely vascular vegetation cover. LAI is leaf area index measured with a LI-COR LAI-2050 Plant Canopy Analyzer before leafing and after leafing. LAI measurements taken before leafing at the wetland site and the valley site were 2.12 and 2.33, respectively. With the foliage fully leafed, the LAI was 3.97 at

the wetland site and 2.66 at the valley site. LAI during the leafing period was linearly interpolated. With limited deciduous vegetation cover at the peatland site, the before and after leafing LAI values were averaged, giving a value of 0.63. C_{maxl} is the maximum leaf conductance (m d^{-1}). The vegetation cover at the wetland site is dominated by woody shrubs and *Carex* spp. A value of 885.6 m d^{-1} was used for C_{maxl} at the wetland site, which is the mean value found from a comparable subarctic marsh (Lafleur, 1988). The dominant plant cover at the valley site is *Picea mariana* and a C_{maxl} of 457.9 m d^{-1} was used, which is a common conifer value (Körner, 1994). C_{maxl} of the evergreen shrub at the peatland site is 285.1 m d^{-1}, a value found for *Ledum* (Lafleur and Schreader, 1994). The calculated vascular plant r_{cmin} values agree with the r_{cmin} footprint at Skeeter Lake located approximately 100 km north of Yellowknife, Northwest Territories (Spence and Rouse, 2002). ET calculations at the peatland site for nonvascular plants and vascular plants were calculated separately with their respective r_{cmin} values and the two resultant ET datasets were averaged by weighting the fraction of nonvascular and vascular plant covers.

The conductance functions are described in Verserghy et al. (1993):

$$f(K\downarrow) = \max\left(1, \left(\frac{500}{K\downarrow} - 1.5\right)\right) \qquad (12)$$

K↓ is incoming solar radiation measured at nearby Landing Lake with a LI-COR 200 pyranometer, and,

$$f(D) = \max\left(1, \frac{D}{5}\right) \qquad (13)$$

the resultant mean r_c was $1.1\text{x}10^{-2}$ d m^{-1} for the peatland vascular cover, $2.5\text{x}10^{-4}$ d m^{-1} for the peatland lichen cover, $2.8\text{x}10^{-3}$ d m^{-1} at the valley site and $1.1\text{x}10^{-3}$ d m^{-1} at the wetland site.

Parts of the peatland and wetland were flooded from the snowmelt period to the end of the field season. To find the potential ET (PET) for these locations, the Penman Combination equation (1948) was used:

$$PET = \frac{\Delta k_c Q^* + \gamma E_A}{\Delta + \gamma} \quad (14)$$

where k_c is a unit converter from MJ m^{-2} d^{-1} to mm d^{-1} (k_c=0.408). E_A (m d^{-1}) is the mass transfer from a Dalton-type equation (1802):

$$E_A = f(u)D \quad (15)$$

where f(u) is the wind function (i.e. vapour transfer function) in mm k Pa^{-1} d^{-1}. Here, the Penman derived f(u) was used:

$$f(u) = 2.63(1 + 0.537u_2) \quad (16)$$

where u_2 is wind speed at a reference height of 2 m (m s^{-1}). u measured at a height of 3.4 m from the wetland station was standardized to the reference height of 2 m with the following equation:

$$u_2 = u_m \frac{\ln(z_2 - 0.67h_c) - \ln(0.123h_c)}{\ln(z_m - 0.67h_c) - \ln(0.123h_c)} \quad (17)$$

u_m is measured wind speed (m s^{-1}), z_2 is the desired wind speed reference height (m), h_c is height of canopy cover (m, see sections 3.1 to 3.3), and z_m is actual instrument height (m).

The daily mean evapotranspiration loss was prorated between ET and PET based on fraction of non-flooded and flooded areas. These fractions were determined from ponded water records noted during soil moisture and frost table surveys. There was surface ponding at the

peatland and wetland sites during the study period and thus both potential (flooded area) and soil ET were calculated at these sites.

4.5.7 Observed Storage Change

Observed change in storage, ΔS_o was calculated using the method described in Spence and Woo (2006):

$$\Delta S_o = \Delta S_u + \Delta S_s = \Delta\theta\left[z(t) - z_w(t)\right] + s_y\left[(z_w(t) - z_w(t-1)\right] \qquad (18)$$

where ΔS_u and ΔS_s are unsaturated and saturated storage change (mm), respectively. For ΔS_u, $\Delta\theta$ is the daily change in soil moisture content as calculated from half-hourly soil moisture data recorded with the ECH$_2$O-TE sensors. The sensors were calibrated with site specific soil samples at the end of the field season. $[z(t)-z_w(t)]$ is total unsaturated soil thickness where z (mm) is based on total thaw depth or total depth to clay due to the limited movement in fine grained soil, whichever is reached first. The peatland site has unsubstantial clay cover, the depth to clay at the valley site was averaged to 0.20 m and at the wetland site, 0.40 m. The water table depths ($z_w(t)$, mm) were measured at the pipes as per discussion in section 4.5.4. At each site, two wells (one at edge of site and one in middle of site) had continuous half-hourly water table level measurements from Solinst Leveloggers. When the soil column was saturated, all the soil pores were filled with water (the space occupied by air bubbles was assumed to be small and ignored here) and unsaturated storage would be zero. For ΔS_s, s_y for the sites are listed in Table 3.1. The term $[z_w(t)-z_w(t-1)]$ represents daily change in thickness of saturated zone (mm). Continuous (every half hour) water table elevation data recorded by Solinst Levelogger described in section 4.5.4 were averaged daily.

4.6 Ground Heat Flux into the Ground

Total ground heat flux into the ground (Q_{gf}) from heat conduction from the soil surface (Q_{gs}) and surface water ponding (Q_{gp}) along with heat advection from flowing water (Q_{gw}) were calculated by modifying the method described in Woo and Xia (1996). Refreezing of infiltrated snowmelt water (or infiltrated rain water) releases latent heat (Q_{fz}) and this can be determined using the method described in Shirazi et al. (2009). The combination of the two methods give the following Q_{gf} equation:

$$Q_{gf} = \underbrace{K_T \left.\frac{dT}{dz}\right|_{surface}}_{conduction(Q_{gs},Q_{gp})} + \underbrace{c_w \, \Delta T \frac{dF}{dt}}_{advection(Q_{gw})} + \underbrace{\frac{\lambda_f V_w \rho_w}{t_o}}_{advection(Q_{fz})} \qquad (19)$$

where all the above Q_{gf} terms are in MJ m^{-2} d^{-1}, K_T is calculated with equation 9, dT/dz is temperature gradient from surface soil and ponded water to the thawing front. The soil temperature was continuously recorded by the ECH_2O sensors, ponded water temperature was recorded with Onset HOBO StowAway Tidbit temperature loggers, and a thawing front temperature of 0ºC was used. c_w is volumetric heat capacity of water (J m^{-3} K^{-1}), ΔT is temperature difference between flowing water and the frozen ground. Snowmelt runoff temperature was measured with a Solinst Levelogger at the soil covered bedrock inlet to the valley site, and was assumed to represent all bedrock runoff temperatures. Lake 690 water temperature was also recorded with the aforementioned Levelogger used for lake storage. dF/dt is flow rate (m^3 d^{-1}). The total inflow water was divided over the dynamic area affected by moving surface water. Not all inflowing water was infiltrated into the ground and some energy would be lost to the atmosphere (e.g. through evapotranspiration) and therefore it should be recognized that potential Q_{gw} was being calculated. However as results will show, when large

heat content was available, there remained ample amount of energy to be transferred into the frozen ground. λ_f is the latent heat of fusion of ice (MJ kg^{-1}), v_w is volume of water per unit area (m^3 m^{-2}), and t_o is infiltration opportunity time (day). The Q_{fz} equation assumes all infiltrated water freezes. Infiltrated meltwater may warm the frozen soil, but not necessarily thaw it (Shirazi et al., 2009). Q_{fz} is time dependent and is more influential in winter and spring when the thawing front is at or near the ground surface and could be negligible at other times when the thawing front is deep. Energy released from refreezing of infiltrated meltwater was not calculated since soil moisture and frost table surveys started after all snow had melted.

Similar to ET and PET, the total Q_{gf} energies available to the frozen ground needed to be partitioned based on the fraction of non-flooded and flooded areas (ponded or flowing) at the sites over time. This was not needed at the valley site since it was flooded only briefly during the snowmelt runoff period. Positive values of Q_{gs} began on April 30 at the peatland site, May 5 at the valley site and May 17 at the wetland site.

4.7 Modified Péclet Number for Northern Wetlands

The Péclet number (Pe) concept has been adopted in many disciplines, and used to quantify landscape spacing of first-order valleys (e.g. Perron et al., 2008) to hillslope subsurface flow (e.g. Lyon and Troch, 2007). Its wide usage is because it can translate often qualitative findings to dimensionless quantitative numbers that can be usefully inputted into computer models. The Pe has also been used to describe relative influences of advective and diffusive energies geothermal processes (Stüwe, 2007):

$$Pe = \frac{u_a l}{k_d} \qquad (20)$$

where u_a is advection rate (m s^{-1}), l (m) is the u_a characteristic length scale and k_d is diffusivity (m^2 s^{-1}). When Pe=1, both advection and diffusion are equally important to a process, when Pe>>1, advective process dominates the process and when Pe<<1, diffusive process is the dominant factor. The Péclet number concept was modified (mPe) in this thesis to find a dimensionless number to represent the relative influence of total advective energy versus total conductive energy at northern soil filled areas:

$$mPe = \frac{\sum Q_{gw}}{\sum Q_{gs} + \sum Q_{gp}} \qquad (21)$$

Thus, the mPe will discern the dominant ground heat source(s) thawing the frozen ground at each site.

4.8 Statistical Analyses

To extract information and patterns from the collected data, the following analyses were used: (1) boxplots for visualization of median and interquartile range changes over time. The outliers (i.e. 1.5 to 3 interquartiles from the end of the 25th and 75th percentile) and extreme outliers (more than three interquartiles from the end of a box) are also graphed; (2) scatterplots for visualization of potential relationships between two variables; and, (3) Spearman rank correlation coefficient (r_s) to determine correlation of soil moisture and frost table depth from each of the surveys:

$$r_s = 1 - \frac{6\sum d_i^2}{n(n^2 - 1)} \qquad (22)$$

where d_i is the rank difference between soil moisture and frost table from the i^{th} survey grid and n is the number of survey points. This nonparametric r_s was used as some datasets were not normally distributed even after log transformation. Measurements where the ground thawed ≥1 m and/or completely were excluded from the correlation analysis.

CHAPTER 5:

SHALLOW SOIL MOISTURE AND GROUND THAW INTERACTIONS

This chapter describes the soil moisture and frost table patterns observed at the three study sites. A total of 16 soil moisture and frost table surveys were done at the peatland site, 14 at the valley site and 7 at the wetland site. Fewer surveys were completed at the wetland site because the snowmelt period took longer than the other two sites due to >0.30 m of accumulated aufeis beneath the snow pack.

5.1 Shallow Soil Moisture

5.1.1 Peatland Site

Soil moisture decreased over the field season at the peatland site. The median soil moisture was 70% on 9/10 May (the first survey was over the span of two days due to logistics) and decreased to 26% on 9 July. Thus, the peat surface dried on average 0.7% per day (Table 5.1). Overall soil moisture decreased over time as the site became drier, except for surveys following rainfall events on 22 May, 24 June and 25 June (Table 5.1 and Figure 5.1a). No outliers (defined as values ≥1.5 interquartiles from the 25th or 75th percentiles) were observed except on 23 June and 9 July. Two outliers were recorded on 23 June and six were observed on 9 July.

Surface water flowed toward the north side of the peatland and the main outlet at the northwest portion of the site. The largest water source was a soil covered bedrock channel northeast of the peatland site that flowed westward toward the main outlet (Figure 4.1a). The observed flow routes matched the locations with the wettest soils. The wettest conditions at the

peatland site occurred during and immediately after the spring freshet in May (Figure 5.2; 9/10 May to 17 May). After freshet peak flow passed, many of the previously inundated hummock tops began to dry as ponded water levels receded. Many of the remaining flooded and saturated locations observed thus were hollows. The flooded and saturated areas shrunk as summer progressed. The outer edges and the south end became drier than the rest of the site. Re-wetting was observed following rain events (e.g. 23 June and 27 June events).

Table 5.1: The median soil moisture (SM) and frost table depth (FT) from all survey dates. Frost table depths ≥1 m were removed from the statistics.

Peatland			Valley			Wetland		
	Median SM (%)	Median FT (m)		Median SM (%)	Median FT (m)		Median SM (%)	Median FT (m)
9&10-May	70	0.09						
13-May	59	0.12	12-May	19	0.09			
15-May	57	0.13	15-May	19	0.09			
17-May	53	0.14	17-May	19	0.10			
19-May	49	0.16	19-May	16	0.10			
21-May	44	0.17	21-May	17	0.12			
23-May	51	0.18	23-May	18	0.12			
25-May	44	0.19	25-May	17	0.13			
27-May	43	0.21	27-May	15	0.14			
29-May	41	0.21	29-May	15	0.15	28-May	75	0.11
1-Jun	39	0.23	2-Jun	16	0.15	30-May	61	0.12
4-Jun	38	0.24	4-Jun	14	0.16	3-Jun	60	0.13
23-Jun	24	0.29	20-Jun	6	0.24	6-Jun	60	0.14
27-Jun	27	0.30	26-Jun	7	0.31	26-Jun	32	0.24
5-Jul	27	0.33	4-Jul	6	0.37	4-Jul	30	0.27
9-Jul	26	0.34				8-Jul	30	0.29

5.1.2 Valley Site

The median soil moisture at the valley site decreased over time from 19% to 6% over 53 days (12 May to 4 July, Table 5.1). Valley soils thus dried at an average rate of 0.2% per day (Figure 5.1c). Outliers were observed on 11 of the 14 surveys and extreme outliers (more than three interquartiles from the end of a box) were found on six surveys. Only one of the 91 survey grids was flooded throughout the study – it flooded on 12-17 May (Figure 5.3). The soil moisture patterns appeared to be organized. For instance, on 27 May, 29 May, 2 June and 4 June, grids with soil moisture ranging between 20 and 40% were often adjacent to one another in the southern part of the site.

5.1.3 Wetland Site

The wetland site dried from a median of 75% on 28 May to 30% on 8 July (Table 5.1, Figure 5.1e). The average rate of drying was 1.1% per day. The wetland site had higher median soil moisture in late-May and early-June than the peatland site, but the values were similar in the rest of June until the end of the field season (Figure 5.1). No outliers in soil moisture were measured at the site.

The flooded area shrunk over the study period (Figure 5.4). The largest flooded area was located in the middle of the wetland where it widens in the SE direction. Other flooded areas were located along stream tributaries and distributaries channeling Lake 690 inflow through the site.

5.2 Frost Table Depth

5.2.1 Peatland Site

The median frost table depth increased over the study period as did the range (Figure 5.1b). There were few outliers in May, and the number of outliers and extreme outliers increased throughout the field season. The median thaw depth increased from 0.09 m on 9/10 May to 0.34 m on 9 July (i.e. 4 mm d^{-1}). If all sample locations are considered, the median thaw depth increased from 0.09 m to ≥1.0 m (i.e. ≥15 mm d^{-1}, Table 5.1).

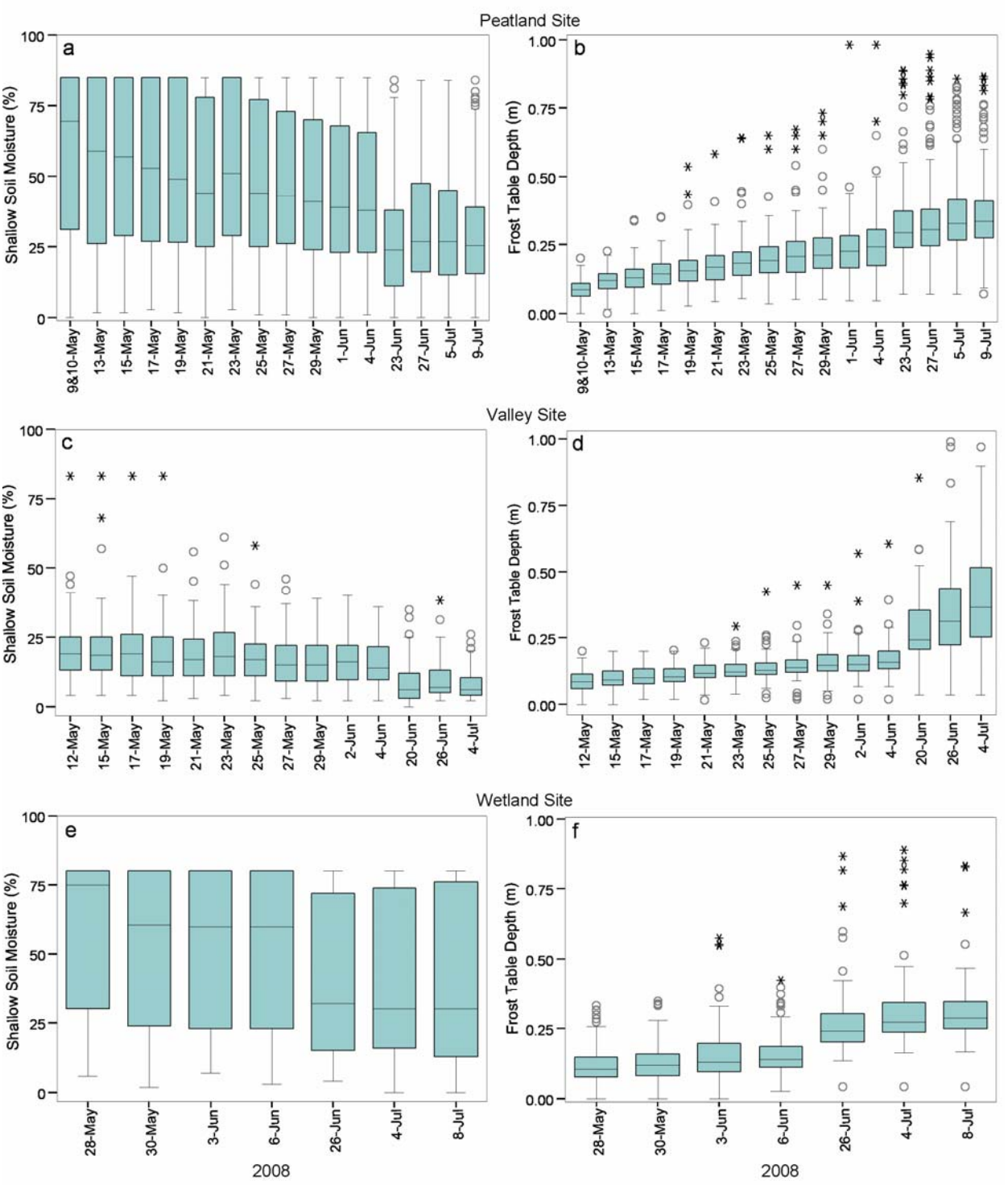

Figure 5.1: Boxplots showing range in shallow soil moisture and frost table depth over time. Circles indicate outliers and asterisks indicate extreme outliers. These outliers are natural variability in the dataset rather than measurement errors. Excluded are sample points with ≥1 m frost table depth.

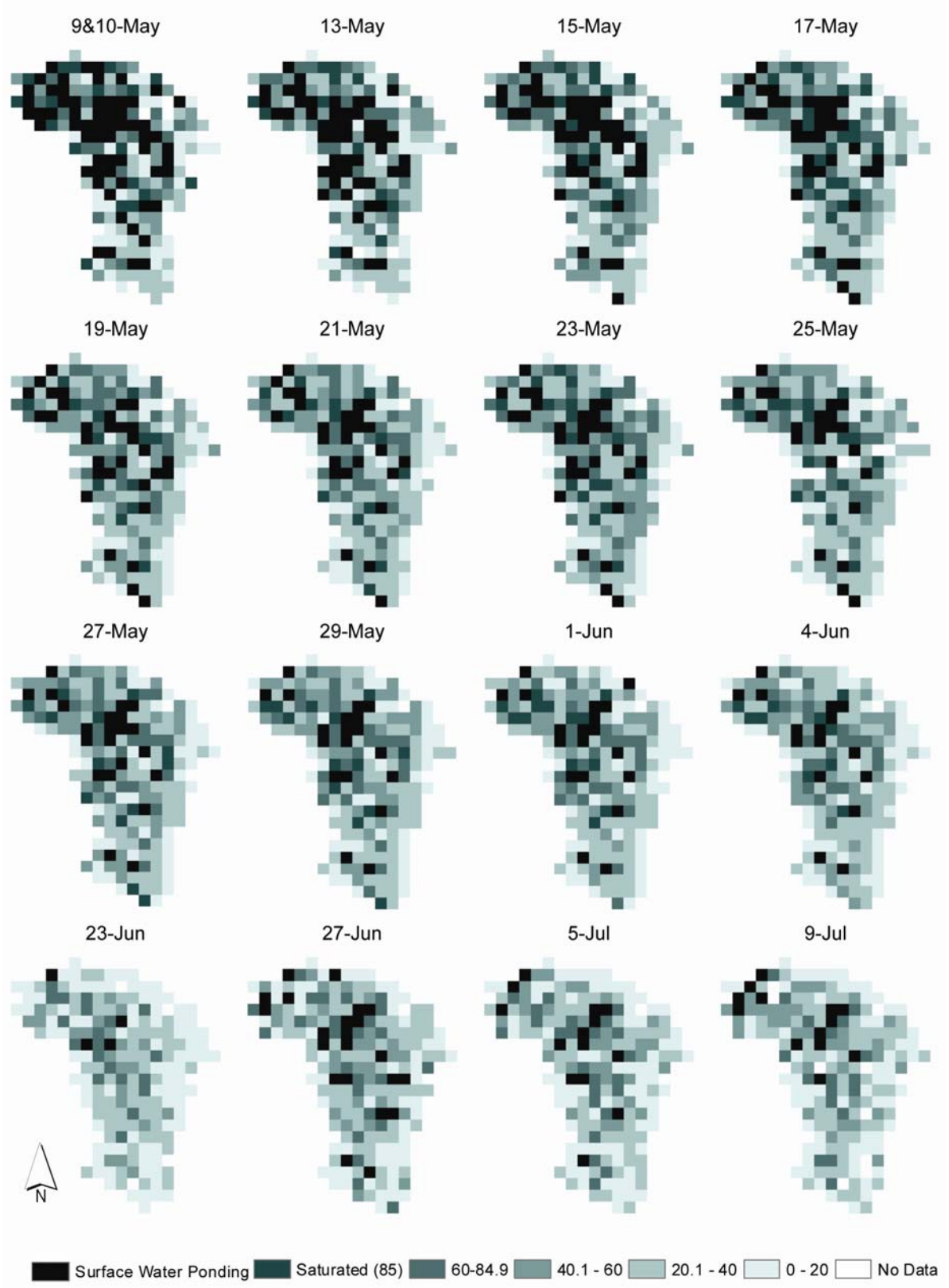

Figure 5.2: Shallow soil moisture surveys at the peatland site. All values are in % and grid cells are mapped at a resolution of 8 m by 8 m from 8 m by 4 m survey data.

Initial ground thaw at all locations was determined by the date the survey point became snow free but this was complicated at locations with flowing or stagnant surface water. The locations with the fastest rate of thaw were randomly distributed across the site in early spring (Figure 5.5, e.g. 15 May), but as thaw progressed, these locations became more clustered in similar areas (Figure 5.5, e.g. 25 May to 9 July). Overlaying the flooded areas from 9/10 May and 13 May over the frost table layer from 9 July reveals almost all of the flooded locations in the spring freshet were the same locations with deepest thaw at the end of the field season (Figure 5.6). Thirty-two percent of the total site area was both flooded and thawed ≥1 m in the above periods. Further analysis of only the flooded grids found 83% of the flooded areas had ≥1 m of thaw by mid-July.

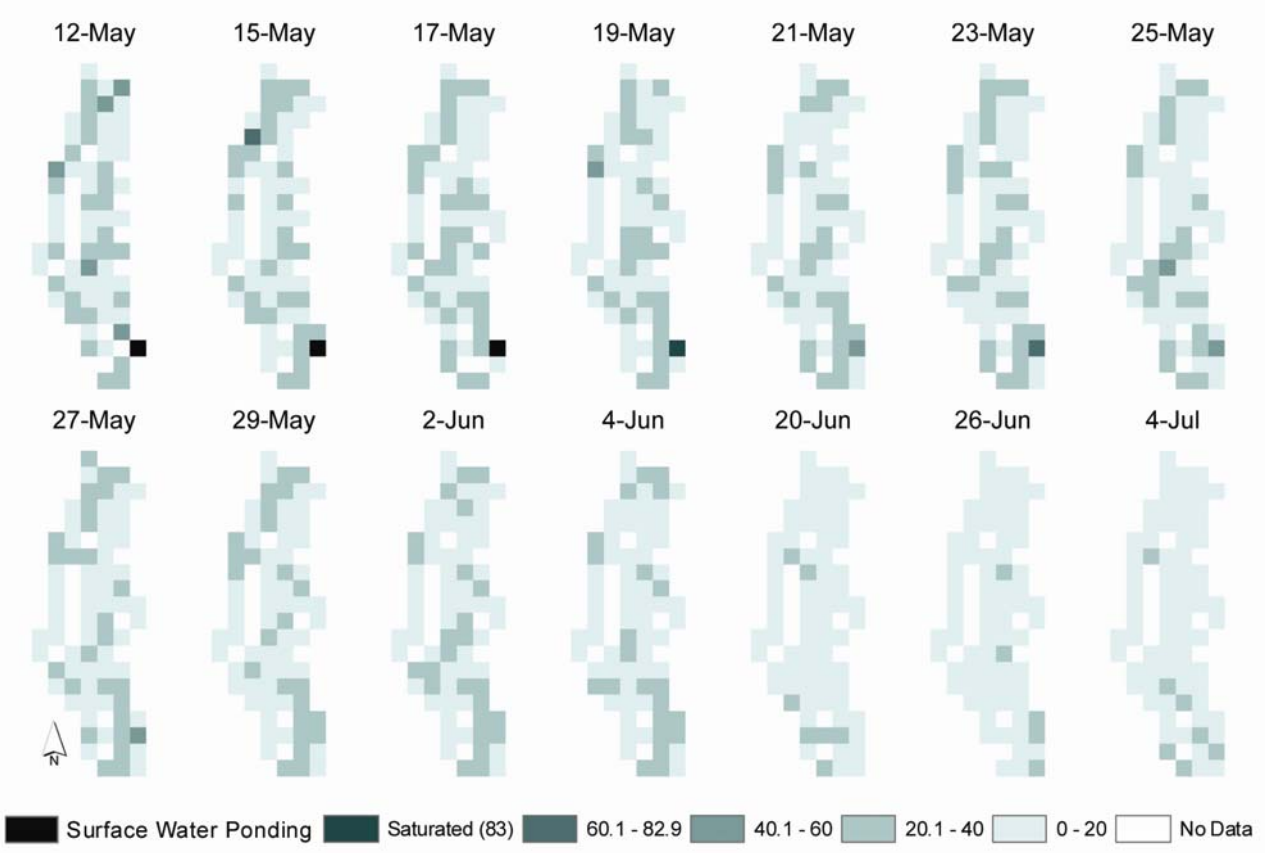

Figure 5.3: Shallow soil moisture patterns at the valley site. All values are in % and survey grids are mapped at a resolution of 2 m by 2 m.

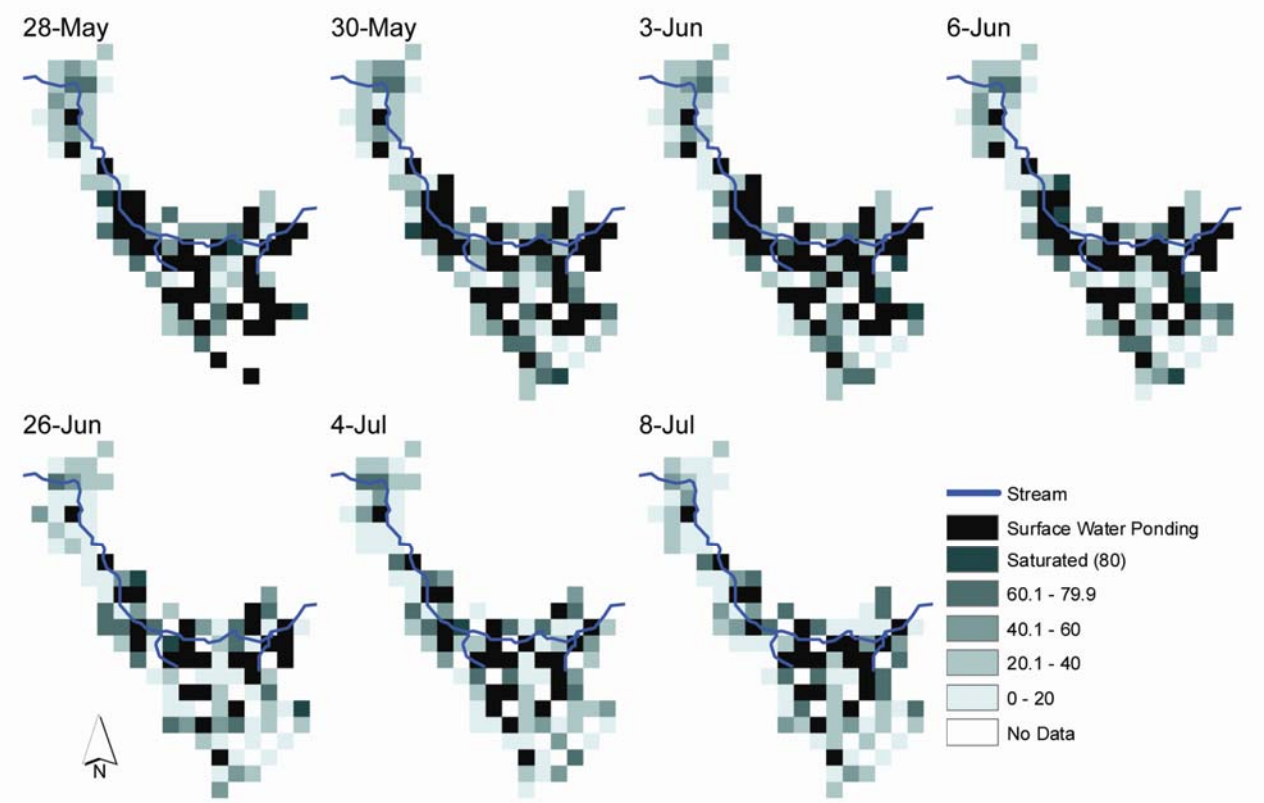

Figure 5.4: Shallow soil moisture patterns at the wetland site. All values are in % and survey grids are mapped at a resolution of 15 m by 15 m.

5.2.2 Valley Site

Similar to the peatland site, the frost table depth range at the valley site increased over the study period (Figure 5.1d). Outliers and extreme outliers were recorded on most sample days. The range of depths measured at this site was smaller than at the peatland until late June. The median thaw depth increased from 0.09 m on 12 May to 0.37 m on 4 July (i.e. 5 mm d^{-1}; Table 5.1). No survey locations thawed ≥1 m at this site by the end of the study period. Up to the 4 June survey, most of the survey points had only thawed <0.20 m (Figure 5.7).

5.2.3 Wetland Site

The interquartile range of frost table depths measured at the wetland site was more constant

over time than at the other two study sites (Figure 5.1f). Over the field season, the number of outliers and extreme outliers increased. The median thaw depth increased from 0.11 m on 28 May to 0.29 m on 8 July (i.e. 4 mm d^{-1}; Table 5.1). If all sample locations are considered, the median thaw depth increased from ≥0.14 m to ≥0.55 m (i.e. ≥10 mm d^{-1}). These rates do not capture the accelerated localized thaw along parts of the surface flow route that thawed ≥1 m while other parts of the wetland were still fully frozen (Figure 5.8). Field observations the following early spring (April 2009) found parts of the flow route were completely thawed even before the onset of snowmelt. Most of the deeply thawed locations on 8 July coincided with locations flooded on 28 May (Figure 5.9). Thirty-four percent of the site was both flooded (28 May) and thawed ≥1 m (8 July). Further analysis of only the flooded grids found 91% of the flooded areas had ≥1 m of thaw.

The temporal patterns show soil moisture became drier and frost table depth increased during the study (Figure 5.10), but the rate of change differed among sites. The slope of line of best fit for frost table depth against soil moisture was -0.006% m^{-1} for the peatland site, -0.02% m^{-1} for valley site, and -0.004% m^{-1} for the wetland site. In addition, localized deep thaw was more accelerated at the wetland site than at the peatland site (Figures 5.5 and 5.8). By 28 May, a large fraction of the wetland already thawed ≥1 m while those locations at the peatland site were not observed until at a later time.

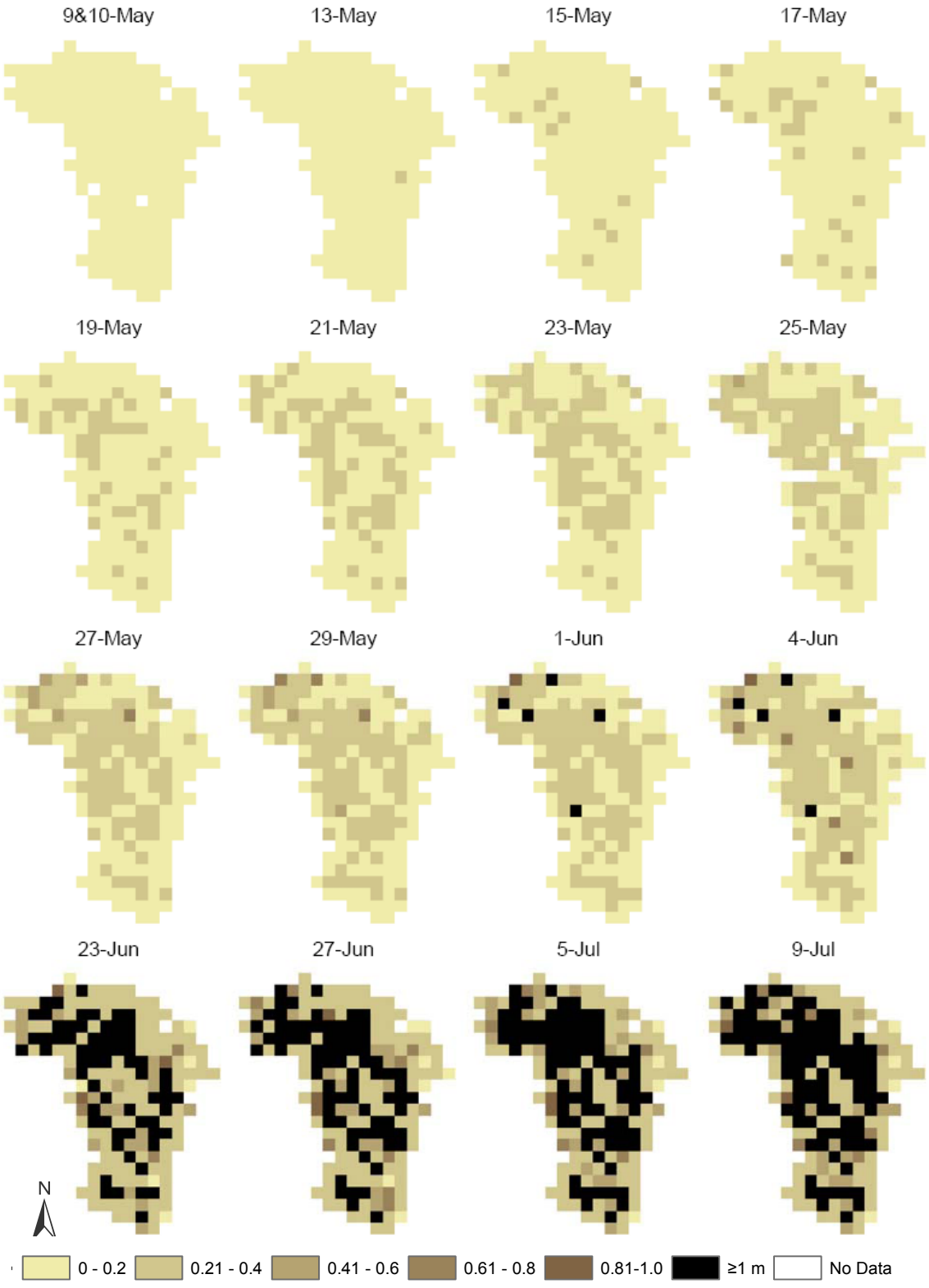

Figure 5.5: Frost table depths at the peatland site. All values are in m and grid cells are mapped at a resolution of 8 m by 8 m from 8 m by 4 m survey data.

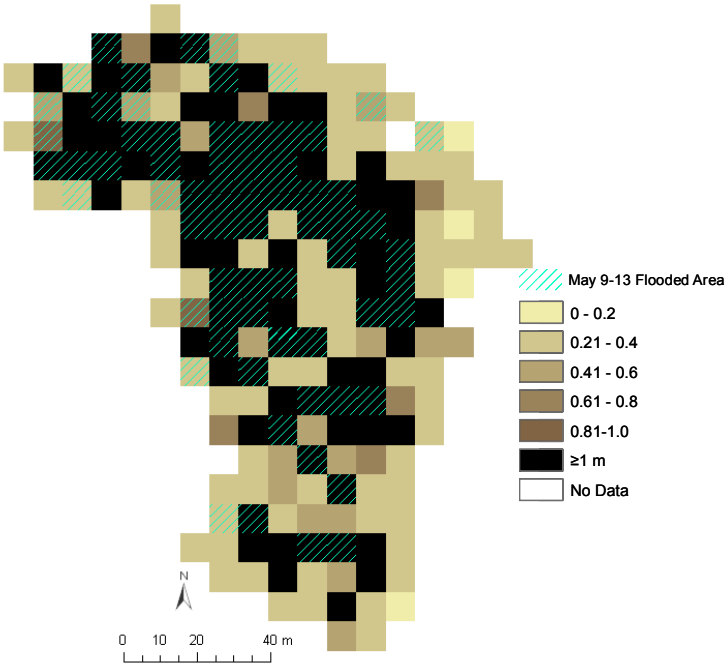

Figure 5.6: Peatland area flooded in early-spring from 9 May to 13 May (hatched grids) overlays the frost table depths measured on 9 July. Any intersecting grids with flooding and ≥1 m thaw indicate those flooded grids were at the same locations as the deepest thaw records. Eighty-three percent of the flooded grids illustrated here had ground thaw >1 m by 9 July. All values are in m and grid cells are mapped at a resolution of 8 m by 8 m from 8 m by 4 m survey data.

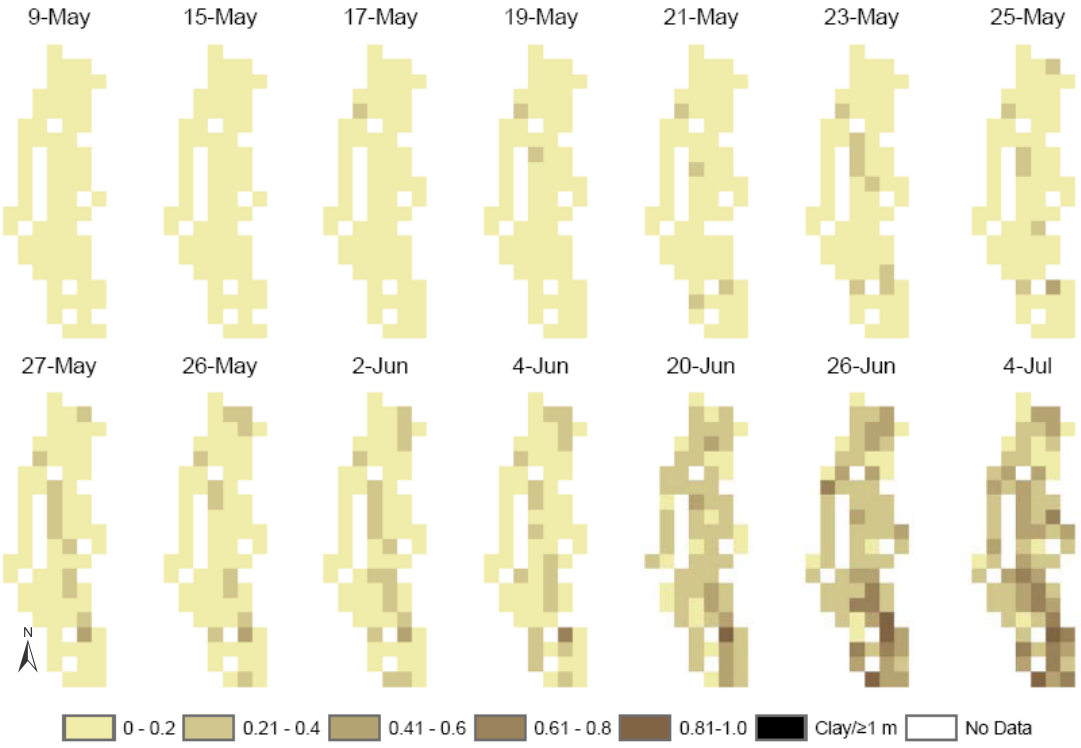

Figure 5.7: Frost table depth at the valley site. All values are in m and survey grids are mapped at a resolution of 2 m by 2 m.

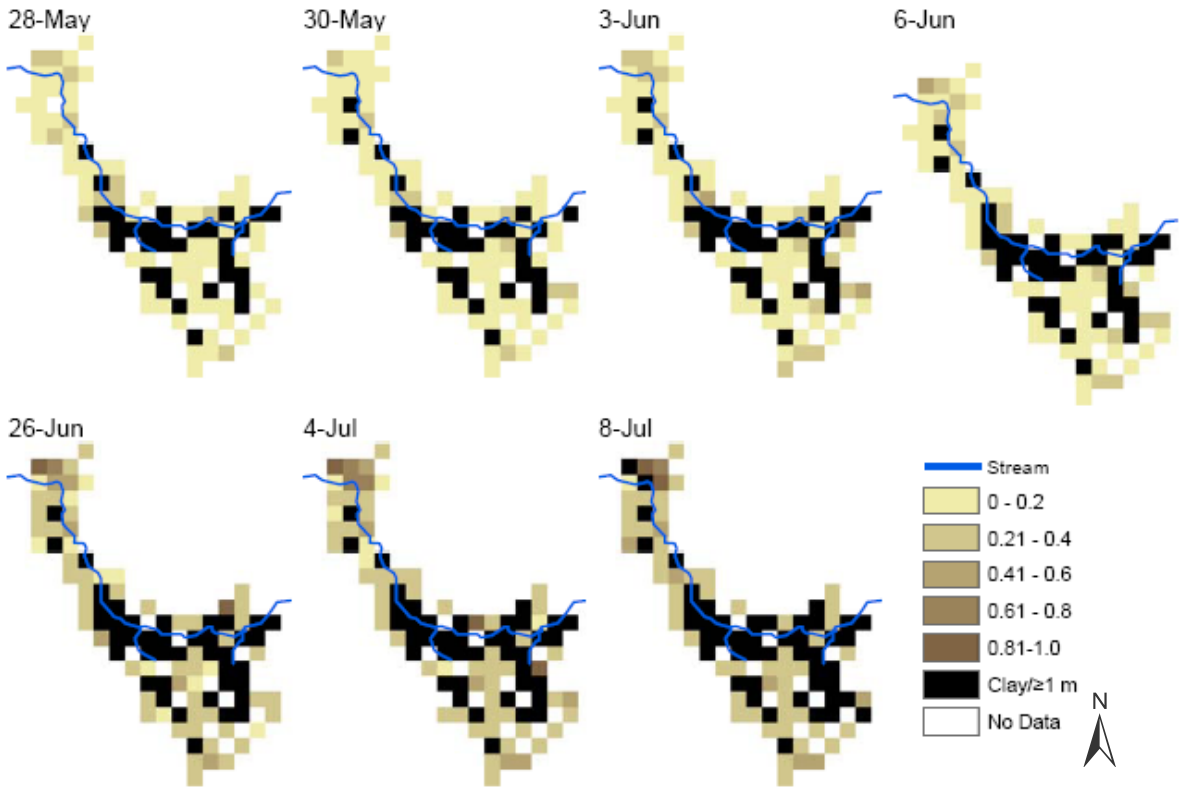

Figure 5.8: Frost table depth at the wetland site. All values are in m and survey grids are mapped at a resolution of 15 m by 15 m.

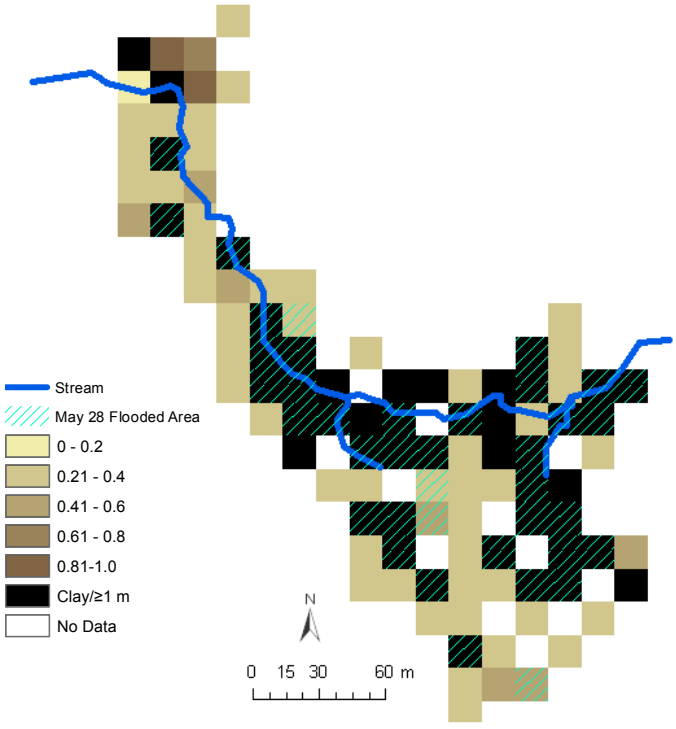

Figure 5.9: Wetland area flooded in the spring on 28 May (hatched grids) overlays the frost table depths measured on 8 July. Any intersecting grids with flooding and ≥1 m thaw indicate those flooded grids were at the same locations as the deepest thaw records. Ninety-one percent of the flooded grids illustrated here had ground thaw >1 m by 8 July. All values are in m and survey grids are mapped at a resolution of 15 m by 15 m.

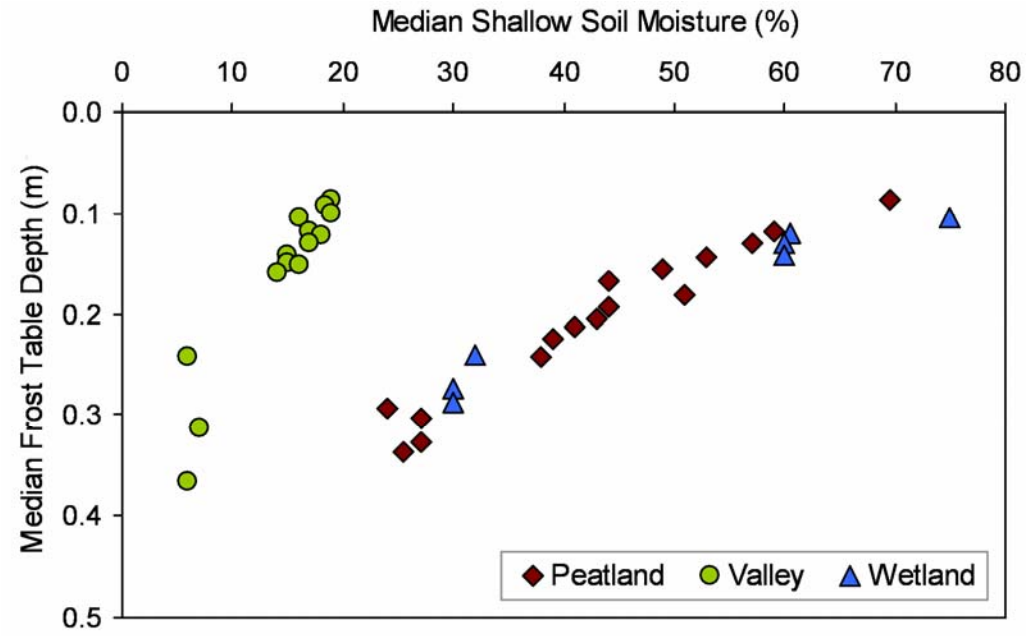

Figure 5.10: The median shallow soil moisture (SM) and frost table depth (FT) from all survey dates revealing the overall temporal patterns. The line of best fit equation through the peatland data was FT=-0.006(SM)+0.5, r^2 was 0.94; at the valley site, FT=-0.02(SM) + 0.4, r^2 was 0.89, and at the wetland site, FT=-0.004(SM) + 0.4, r^2 was 0.95.

5.3 Soil Moisture-Frost Table Interaction

Spatially at the intra-site scale, when the shallow soil moisture at the peatland site was higher, the frost table depth was deeper during individual surveys (Figures 5.6 and 5.11). This spatial pattern is opposite to the temporal data shown in Figure 5.10. Spearman rank correlation coefficient calculations showed soil moisture and frost table were most significantly correlated at the peatland site (Table 5.2; Figure 5.11). The r_s in the peatland increased through the summer to 4 June. Between 4 June and 24 June, the r_s started to decrease and this trend continued until the end of the field season. The r_s from all survey dates were significant at this site except for the last survey on 9 July. The valley r_s values were variable, ranging between negative and positive. Five out of 14 surveys were significantly correlated: 12 May, 15 May, 19 May, 26 June and 4 July (Figure 5.12; Table 5.2). Of these three were negative while two were positive. The r_s from

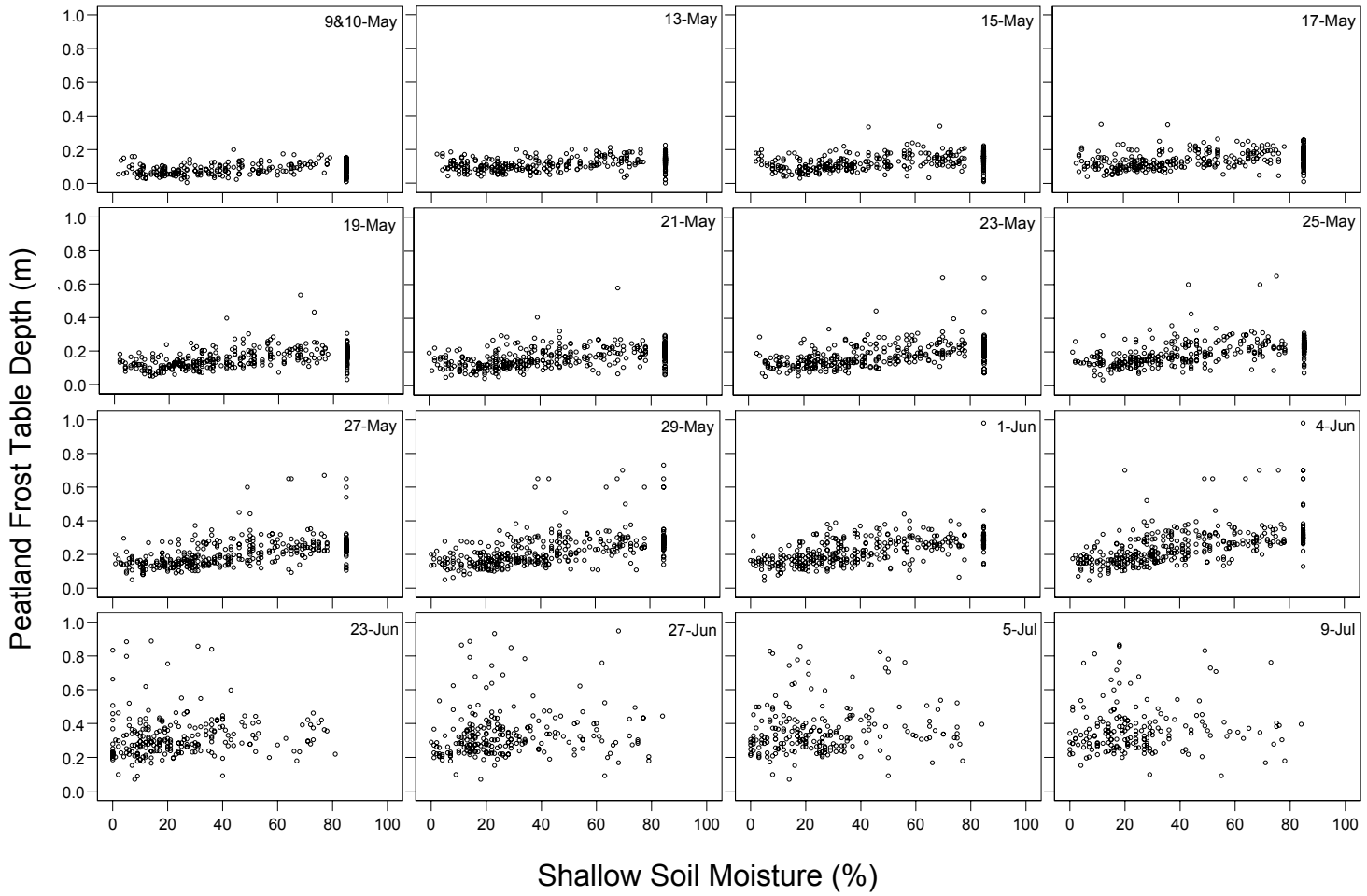

Figure 5.11: Frost table depth and shallow soil moisture from all survey dates at the peatland site. Locations with only seasonal frost were removed from remaining survey graphs once completely thawed and locations with thaw depth ≥ 1 m also removed. Table 5.2 lists Spearman rank correlation coefficients (r_s) and p for each plot.

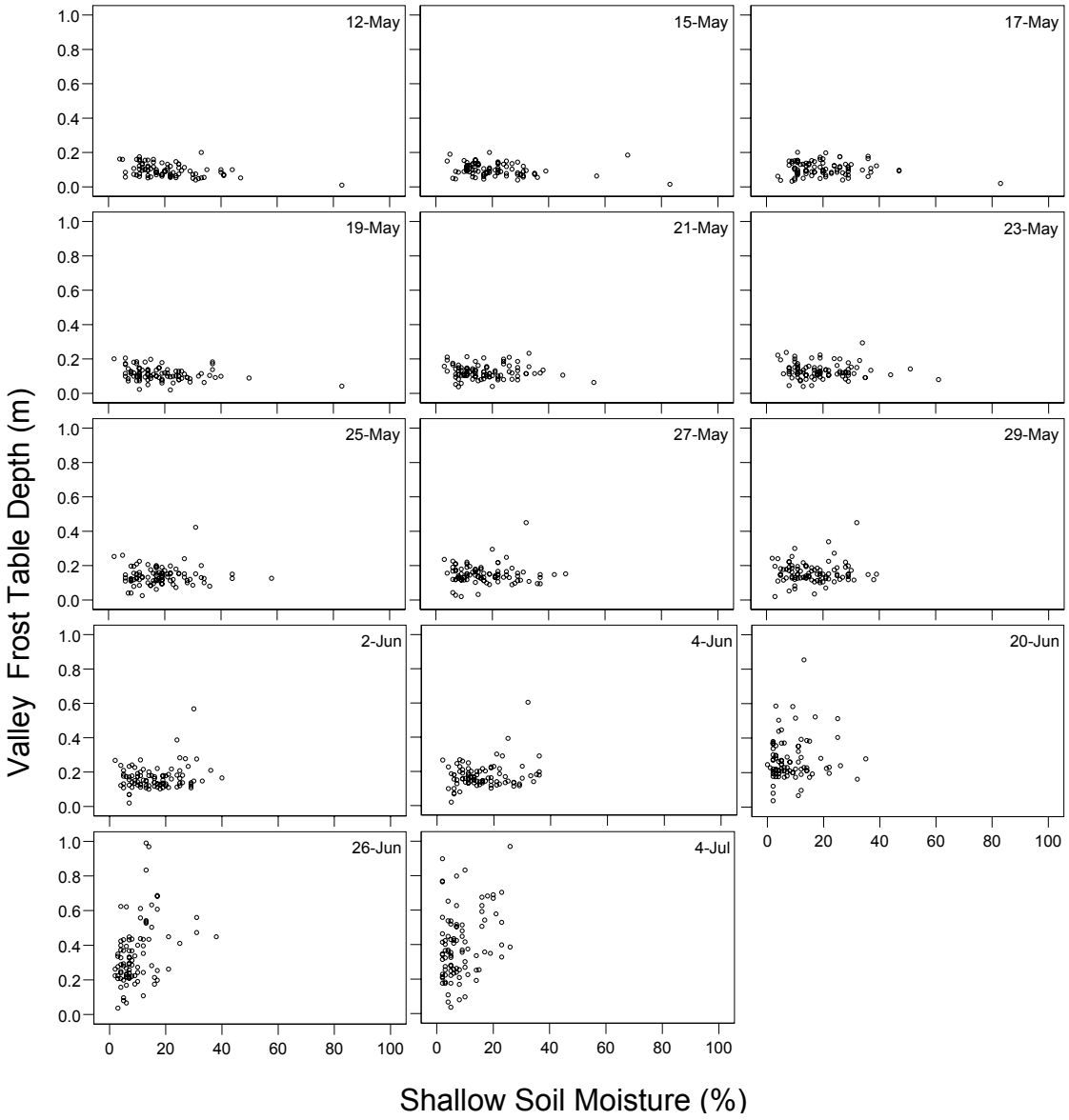

Figure 5.12: Frost table depth and shallow soil moisture of all survey dates at the valley site. Locations with only seasonal frost were removed from remaining survey graphs once completely thawed and locations with thaw depth ≥ 1 m also removed. Table 5.2 lists Spearman rank correlation coefficients (r_s) and p for each plot.

the first four wetland surveys were comparable to the first four surveys at the peatland site. The r_s at the wetland was non-significant starting on 26 June and remained so until the end of the study (Table 5.2; Figures 5.13 and 5.14a).

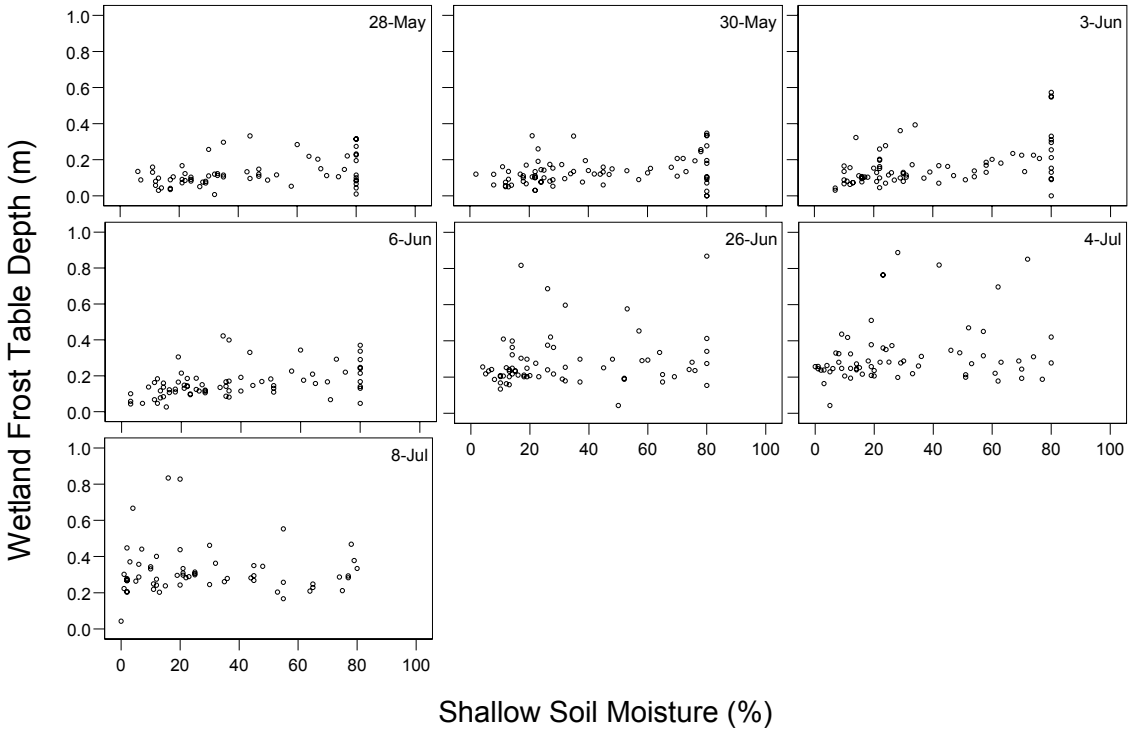

Figure 5.13: Frost table depth and shallow soil moisture of all survey dates at the wetland site. Locations with only seasonal frost were removed from remaining survey graphs once completely thawed and locations or where thaw was ≥1 m. Table 5.2 lists Spearman rank correlation coefficients (r_s) and p for each plot.

There is an overall positive correspondence between r_s and site wetness when all sites were considered (i.e. landscape scale, Figure 5.14b). However, this trend is less obvious when individual landscape units were considered. There was a negative trend of r_s over the median degree of saturation at the valley site. The trend at the two other sites fluctuated from a positive to a negative trend over the degree of site saturation. The r_s at the wetland and peatland sites were highest in the period between the end of snowmelt and before the onset of significant evapotranspiration in the summer (Table 5.2; Figure 5.14a).

Table 5.2: The total number of sample pairs used to calculate Spearman rank correlation coefficient (r_s) between shallow soil moisture and frost table depth for all surveys at the study sites. Bolded *p* values are significant at alpha of 0.05.

Peatland Site

Survey Date	9&10-May	13-May	15-May	17-May	19-May	21-May	23-May	25-May	27-May	29-May	1-Jun	4-Jun	23-Jun	27-Jun	5-Jul	9-Jul
n	352	362	373	375	375	379	379	363	378	378	366	366	242	230	206	183
r_s	0.34	0.42	0.47	0.48	0.59	0.54	0.58	0.61	0.61	0.63	0.63	0.66	0.23	0.21	0.15	0.11
p	**0.000**	**0.000**	**0.000**	**0.000**	**0.000**	**0.000**	**0.000**	**0.000**	**0.000**	**0.000**	**0.000**	**0.000**	**0.000**	**0.002**	**0.034**	0.153

Valley Site

Survey Date	12-May	15-May	17-May	19-May	21-May	23-May	25-May	27-May	29-May	2-Jun	4-Jun	20-Jun	26-Jun	4-Jul
n	80	84	88	89	89	91	90	91	91	91	90	90	90	91
r_s	-0.37	-0.23	-0.04	-0.29	-0.08	-0.10	0.03	-0.10	-0.07	0.07	0.07	0.03	0.40	0.24
p	**0.001**	**0.034**	0.681	**0.006**	0.472	0.334	0.802	0.338	0.529	0.502	0.519	0.785	**0.000**	**0.020**

Wetland Site

Survey Date	28-May	30-May	3-Jun	6-Jun	26-Jun	4-Jul	8-Jul
n	65	78	75	73	68	67	62
r_s	0.36	0.31	0.48	0.50	0.21	0.21	0.06
p	**0.003**	**0.005**	**0.000**	**0.000**	0.084	0.084	0.625

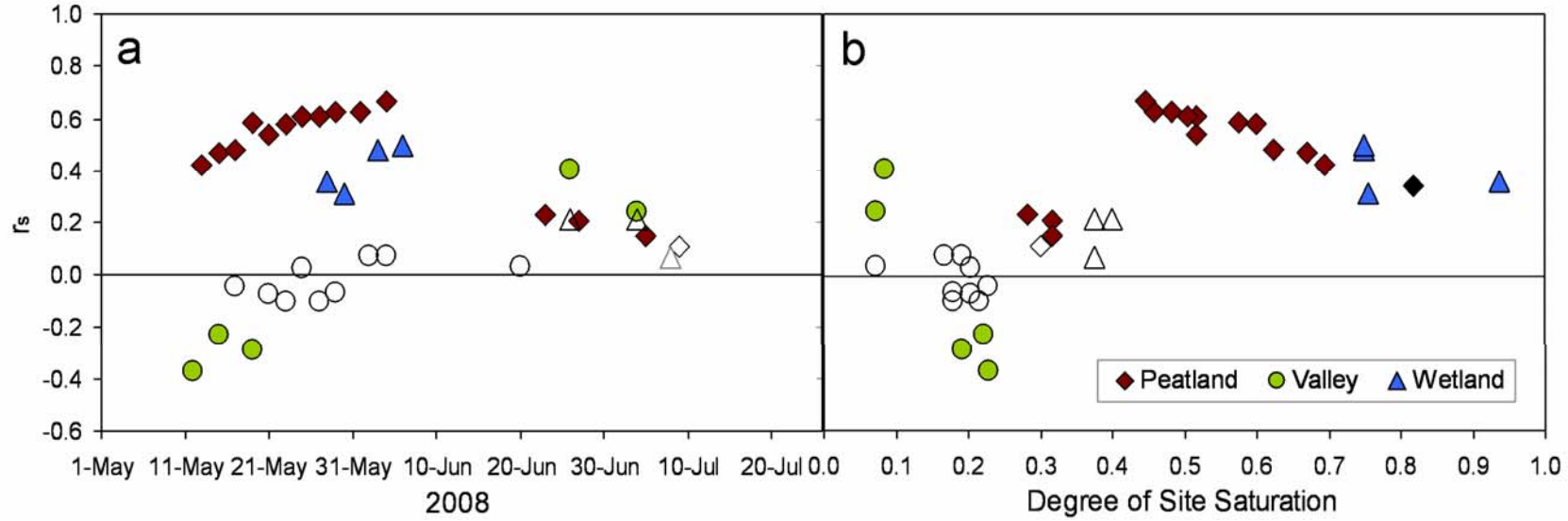

Figure 5.14: The Spearman rank correlation coefficient (r_s) between shallow soil moisture and frost table depth: (a) for all survey dates at the three study sites, and (b) r_s over the sites' median degree of saturation, S (volumetric water content divided by porosity). The line of best fit through data from all three sites is r_s=0.8S-0.08 with r^2=0.42. When a location thawed deeper than 1 m, the grid was removed from the remaining analysis. Closed and open symbols show significant and non-significant r_s at α=0.05, respectively.

5.4 Discussion

5.4.1 Shallow soil moisture – ground thaw patterns and correlations

Temporally, overall soil moisture decreased and frost table depth increased from spring to summer due to seasonal forcings (Figure 5.10). Spatially, deeper summer ground thaw was usually found at wetter soil locations within each hillslope that were prone to spring flooding (e.g. Figure 5.14b). This relationship between soil wetness and ground thaw is comparable to that of Dingman (1971) who studied subarctic footslopes at Glenn Creek in central Alaska and found areas near streams often had more ground thaw than those upslope. Similarly, Nicholson (1978) found "wet lines" (i.e. drainage lines) as marked by surface vegetation often had deeper thaw than drier locations in Schefferville, Québec. When frozen ground thaws, both soil hydraulic conductivity and water storage capacity increase (e.g. Dingman, 1975; Hayashi et al., 2007). Such processes enhance percolation and can facilitate an increase in soil water storage (Dingman, 1975) and create a feedback process whereby ground thaw is enhanced. This study found an interactive link between soil moisture and frost table depth over site wetness that was likely controlled by the feedbacks described above. We have conceptualized this interactive link in Figure 5.15. Similar findings were previously suggested by Carey and Woo (2000) and Wright et al. (2009).

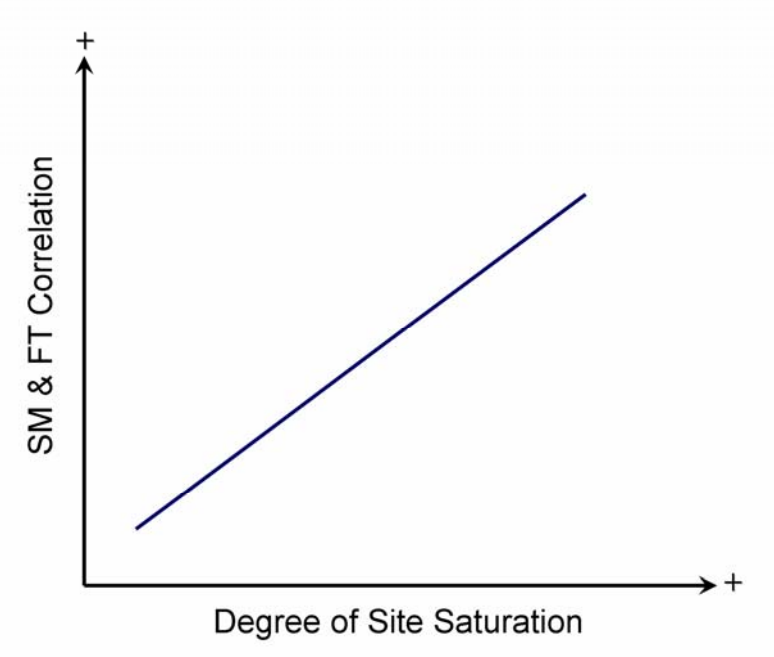

Figure 5.15: Conceptual model illustrating the interaction of soil moisture (SM) and frost table (FT) over space as a function of site wetness. When the site soil moisture is relatively low (e.g. at the valley site), the interaction is more time dependent. When the site soil moisture is wetter (e.g. at the peatland and wetland sites), the interaction becomes more correlated.

Studies from Resolute, Nunavut found ground thaw was inversely proportional to soil ice content where more ice rich organic soils had shallower thaw than polar desert soils due to a prolonged zero-curtain effect at the thawing front (Woo and Xia, 1996; Carey and Woo, 1998a). This zero-curtain influence explains the patterns of thaw observed at the valley site but not at the other two sites. At the wetland site, a large fraction of the ice rich soil site along the surface flow route thawed completely before the site was even snow free. This resulted in a large variance in thaw depth in the spring. However, by early summer, the overall variance in thaw depth decreased as the frost table front became increasingly homogeneous throughout the site. In contrast, the thaw depth at the peatland and valley sites became more heterogeneous over time due to differential thawing over space. Chapter 6 examines the hydrological reasons for the accelerated thaw rate at ice rich locations and the contrasting findings in thaw depth among sites.

The relationship between active soil depth and soil wetness presented here differs from those in temperate regions with a fixed lower impermeable boundary. For instance, Tromp-van Meervald and McDonnell (2005; 2006) found thin soil locations above bedrock were more likely to saturate and contribute to runoff downslopes during low to medium intensity rain events due to the lower local storage capacities. The patterns of wetter surface soils associated with thicker active soils found at Baker Creek were comparable, however, to those observed by Devito et al. (1996) at the southern limit of the Canadian Precambrian Shield, although they were controlled by different processes. They found deeper soils maintained baseflow more than shallow soils and thus kept the water table close to the ground surface. Their work illustrates the importance of hydrological fluxes in maintaining soil moisture that Chapter 6 will examine further.

The relationship between surface soil moisture and ground thaw within individual soil filled units was hysteretic and complex. At the peatland and wetland sites, the highest r_s were recorded in June. This is later than those noted by Wright et al. (2009), who observed higher r_s in the spring in a similar discontinuous permafrost landscape to this study site. When these two sites were extensively flooded during the spring freshet, the soil moisture patterns did not initially reflect the frost table front. The ground thaw rates at the wetland site along and adjacent to the stream as presented especially do not capture the accelerated thaw rate along surface flow paths. Many of these locations thawed ≥1 m by the first survey on 28 May, and were left out of the remaining correlation analysis. As the sites dried over time, the locations that were initially the wettest experienced the deepest thaw. This is reflected in the coincidence of wet surface conditions and deep frost tables in early July (Figures 5.6 and 5.9). When the thaw depth depleted further from the ground surface in the summer, the relationship between deeper ground thaw and soil moisture began to degrade as surface soil moisture became decoupled from ground

thaw processes. The soil moisture-ground thaw correlation was affected by site wetness as illustrated above, but these correlations are dynamic and expected to differ in the spring and fall under a similar site wetness condition. Other hydrological processes, notably the number of heating degree days may have become more influential in determining moisture and thaw patterns as the summer progressed. The above pattern was not present in the drier valley site. In contrast to the wetter peatland and wetland sites, the drier valley site had a more variable correlation pattern with some significant negative interaction between soil moisture and ground thaw in the spring and then some significant positive interaction in the summer. This can be explained because of two phenomena. First, because there was little to no ponding of water on the valley floor, early soil moisture values were not well correlated with ground thaw. As the frost table thawed deeper, the soil moisture decreased whilst the peatland and wetland sites deviated from this response due to contribution of surface water. Second, the shallower thaw depths in the valley meant the thaw front was less decoupled from the surface for more of the study period, and eventually, the wettest sites in the valley became positively correlated with thaw depth. Overall, there was a stronger correlation between soil moisture and ground thaw with increasing site wetness at the landscape scale. This upscaling pattern could be considered comparable to river flow regimes where flow patterns are more spatially diverse at the smaller scale (Gustard, 1992).

5.4.2 Typology, topography and topology

The complex, intra-site soil moisture and ground thaw interactions can be described with Buttle's (2006) T^3 conceptual model of primary first order controls on hydrological response. Typology varied among the sites. The surface soil at the peatland and wetland sites was organic whereas the valley site had thinner organic cover over fine grained mineral soil. The vegetation

at the valley site was believed to have increased snow interception (Pomeroy and Gray, 1995) and transpiration relative to the other two sites as has been shown to occur in other ecozones. These typological differences may have exerted variable hydrological and thermal control on soil water storage and ground thaw, which is further examined in Chapter 6. At the peatland site, most the outer boundary was dry and did not have enough soil water for hydrological connection likely due to the thin soil cover over the bottom of the bedrock slopes that surrounded the site (Devito et al., 1996). This caused the boundary to be hydrologically isolated from the rest of site.

The peatland and wetland sites both had a gentle site topographic gradient while the valley site had a steeper gradient. While there were often clusters of similar soil moisture values adjacent to one another in the peatland, there was little impact on hydrological connectivity unless the soils had high wetness. The valley drained surface runoff out of the site at a fast rate and consequently surface ponding was minimized. The lack of surface depressions at this site also contributed to the reduced potential for surface water storage, which was shown at the other two sites to be important in maintaining soil wetness throughout the study. These findings were comparable to Woo and Winter (1993) who concluded wetland sites tend to have larger and longer duration of surface flooding than upland sites partly due to a lower topographic gradient.

Topology also varied among sites. The peatland and valley sites were soil filled depressions surrounded by exposed bedrock. The wetland site was situated between two lakes and received continuous surface water input. The dominance of vertical and lateral water fluxes in controlling the correlation between soil moisture and position has been previously noted in the literature (Western et al., 2001; Blyth et al., 2004; James and Roulet, 2007). Thus at Baker Creek, each site's topology influenced the amount of surface water input and may have influenced the soil moisture patterns and ground thaw. This idea is explored in detail in Chapter 6.

Rarely is one first order control acting independent of the other two. Figure 5.16 depicts where on Buttle's (2006) T^3 conceptual model each of the three sites fit. Topology controlled the soil moisture and ground thaw interaction at the wetland site. Topological influences decreased at the peatland and valley sites. Instead, the soil and the hollows at the peatland site controlled the site's wetness, and thus, typology and topography were influential at this site. Topography at the valley had the most important influence because of its control on water draining from the site. Though the T^3 template does not directly incorporate climatic forcings, each of the Ts indirectly encompasses climatic influences.

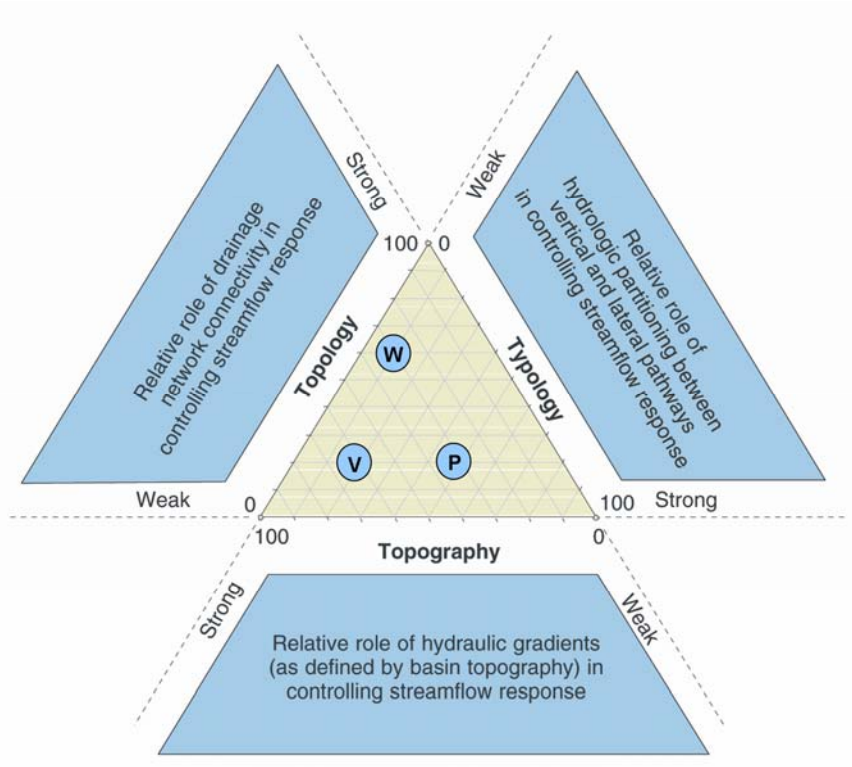

Figure 5.16: The relative influence of topography, topology and typology on the shallow soil moisture and ground thaw interaction. The higher the number in the ternary diagram, the greater the control. P is peatland site, V is valley site and W is wetland site. Modified from Buttle (2006).

CHAPTER 6:

HYDROLOGICAL AND ENERGY CONTROLS ON SHALLOW SOIL MOISTURE AND GROUND THAW INTERACTIONS

This chapter describes the water and energy fluxes at the three study sites. These fluxes are used to explain the patterns in soil moisture and frost table depth reported in Chapter 6.

6.1 Hydrological Fluxes

6.1.1 Snowmelt

The end of winter SWE's (12 April 2008) were 93 mm at the peatland site, 117 mm at the valley site and 61 mm at the wetland site. Snowpack depth measurements were conservative as the mean daily air temperatures from 9-13 April were above 0ºC and some snowmelt and runoff was observed upon arrival to the study site. However, mean daily air temperature dropped below 0ºC on 14 April and did not warm up to 0ºC again until 27 April (Figure 6.1). The snow ripened again on 27 April at all three sites. Most of the snow melted by 4 May at the valley site, contributing 45 mm of water equivalent to the site. At the peatland site, there was an observed increase in snow-free areas with snowmelt on 27 April, occurring first mainly on high hummocks. The majority of snow at the peatland site disappeared by 3 May. Exceptions were some hollows in the middle of the site and along the outer boundary in the dense conifer stands. Total snowmelt into the peatland was 73 mm. Outflow from Lake 690 created an ice layer 0.32 m thick in the wetland. Assuming an ice density of 920 kg m^{-3}, this ice layer amounted to 294 mm of water storage at the wetland site prior to snowmelt. Snow and ice at the wetland site melted first along a surface stream conveying water from Lake 690 across the site (Figure 6.2).

By 30 April, snow at the wetland ablation line thawed to the ice layer. Much of snow and ice cover melted by 13 May, however, patches remained until 21 May. These patches were located in dense shrub and conifer stands, except for locations with surface flow routes. Total snow and ice melt input to the wetland was 185 mm.

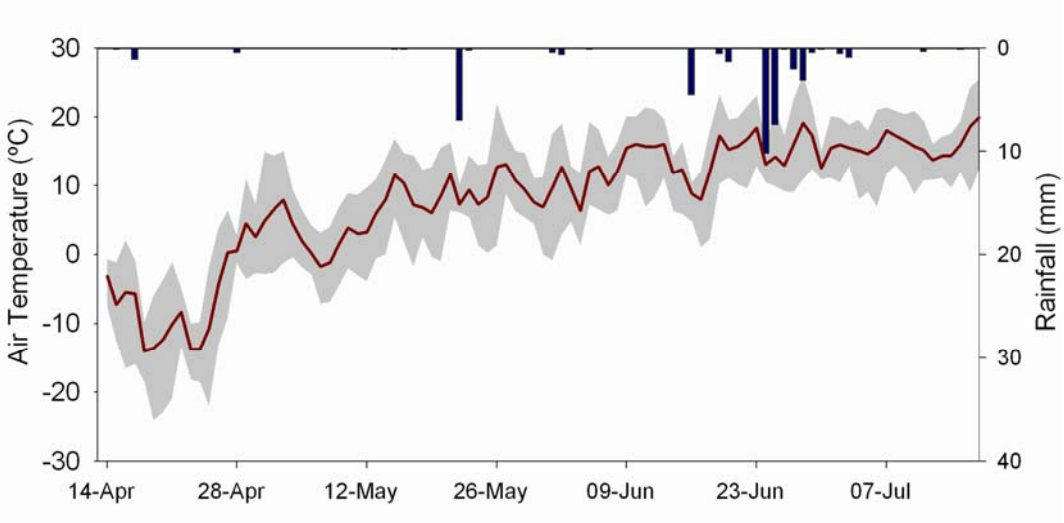

Figure 6.1: Mean daily air temperature (range is shown in grey) and total daily precipitation measured at the wetland climate tower.

Figure 6.2: The wetland site on 6 May 2008 during the snowmelt period. Snow and ice melted at a faster rate along surface runoff routes, while much of the remaining snow covered areas were outside of flow pathways. Photo was taken facing east with Vital Lake (ice covered) in the background.

6.1.2 Rainfall

All three sites were within 1 km from the wetland climate station and thus, rainfall at the peatland and valley sites was expected to be the same as at the wetland site. A total of 42 mm of rainfall fell from 14 April to 17 July (Figure 6.1). The rainfall in May, June and July (full month) were 7, 31 and 15 mm, respectively. The 1961 – 2000 climate normals from the Environment Canada Yellowknife A station are 19 mm, 27 mm and 35 mm for the months of May, June and July, respectively, which indicates May to July 2008 was relatively dry, i.e. 65% of normal.

6.1.3 Inflow

Bedrock runoff was observed on 12 April and 13 April during a warm spell. When the mean daily air temperature dropped back to below 0ºC on 14 April, bedrock runoff ceased and did not occur again until 27 April. After that, it flowed at a mean daily rate of 14 mm day^{-1} (Figure 6.3) when the mean daily temperature reached >0.2ºC (Figure 6.1). The highest mean daily rate was measured on 30 April with 19 mm day^{-1} of flow. For the bare bedrock weirs, the last date with flow through all three was 3 May. The 22 May rainfall filled many bedrock micro-depressions and initiated bedrock runoff at some locations, however, the flow depth and volume were immeasurable. Rain on 24-25 June led to widespread bedrock runoff at all three sites. A mean daily inflow rate of 12 mm and 0.4 mm were measured from the three bedrock weirs on 24 June and 25 June, respectively. Using these rates, extent of bedrock coverage, and site area to model the two day total I_{bss} showed 17 mm of input to the peatland site, 34 mm into the valley site and 12 mm into the wetland site.

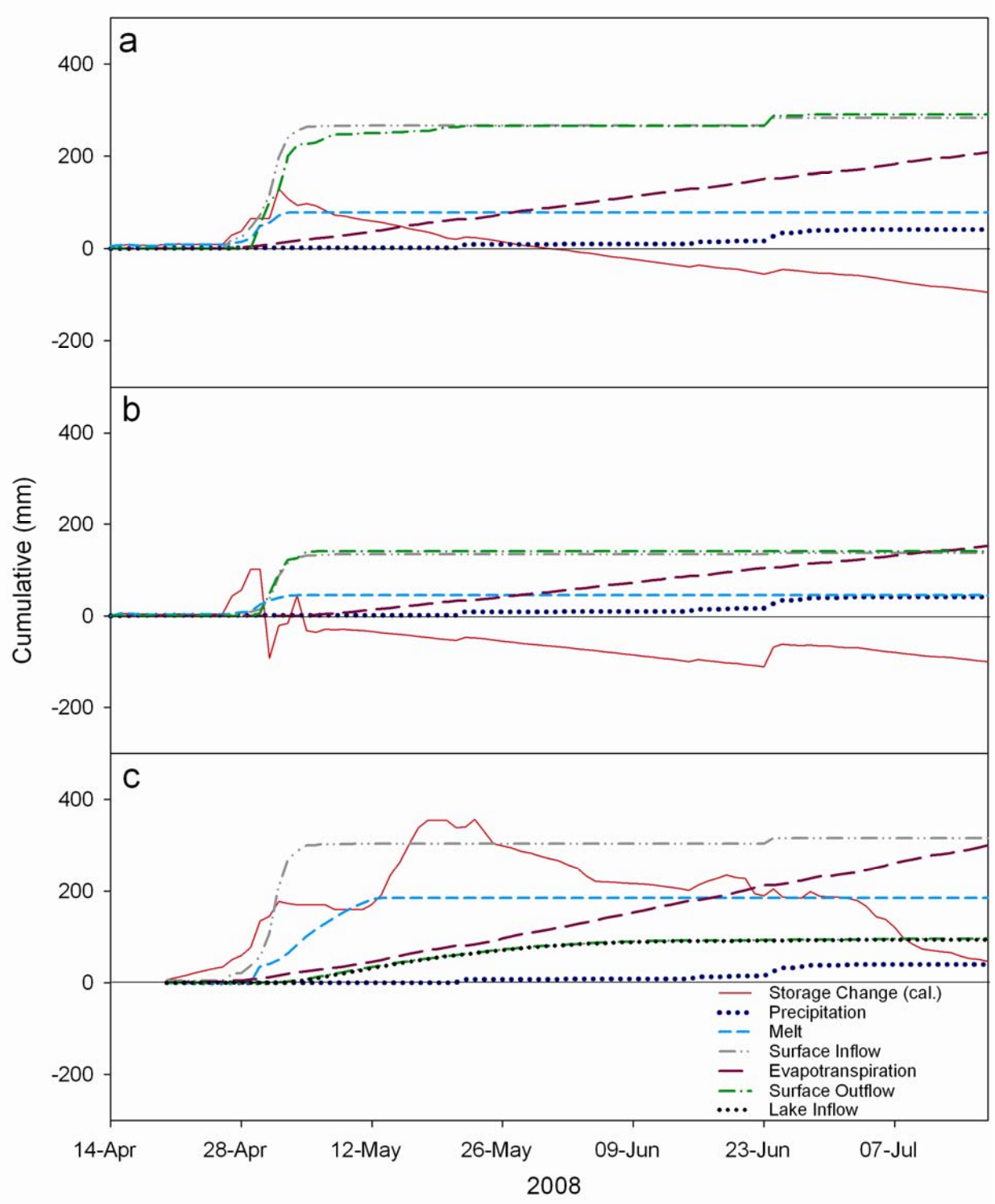

Figure 6.3: Cumulative water budget for the (a) peatland, (b) valley, and (c) wetland sites (mm per unit area) for 14 April to 17 July 2008. For display purposes, surface inflow and outflow values are one-tenth of actual at the valley site (i.e. ~137 mm of cumulative inflow shown in graph is representing the actual ~1370 mm). Surface outflow and lake inflow are one-hundredth of actual at the wetland site.

Inflow from Lake 690 was recorded starting on 20 April once a lake level pressure transducer was installed. It is assumed there was continuous inflow from Lake 690 during the winter because of the icing across the wetland site. The mean daily discharge from Lake 690 during the study period was $3.5x10^3$ m^3 day^{-1} (Figures 6.3c and 6.4). The mean was skewed by the high flow that occurred in May ($8.4x10^3$ m^3 day^{-1}) compared to June ($1.4x10^3$ m^3 day^{-1}) and the days it was measured in July ($2.2x10^2$ m^3 day^{-1}). Lake 690 discharge decreased drastically when the lake level dropped below its natural outlet dam level in mid-June and a large decrease in discharge was observed from 6 June to 14 June. Most of the discharge water flowed through holes in the debris dam. At the wetland site, there was thawed ground along the surface flow pathways. The peatland site had approximately two orders of magnitude less cumulative lateral surface water input than the wetland site whereas the valley site had approximately one order of magnitude less lateral surface water input than the peatland site (Figure 6.4).

Subsurface inflow at the wetland site was negligible relative to the large quantity of surface inflow. The mean daily rate was 0.005 mm day^{-1}. At the peatland site, the extensive bedrock surrounding the site prevented significant subsurface input into the site. The available measurements from the valley site when the pipes were not ice jammed, or had measurable water table depth revealed subsurface flow to be low. Its estimated maximum subsurface flow rate was 0.04 mm day^{-1} since the water table position was mostly within the deeper fine mineral soil which has a K of 10^{-8} to 10^{-9} m s^{-1}.

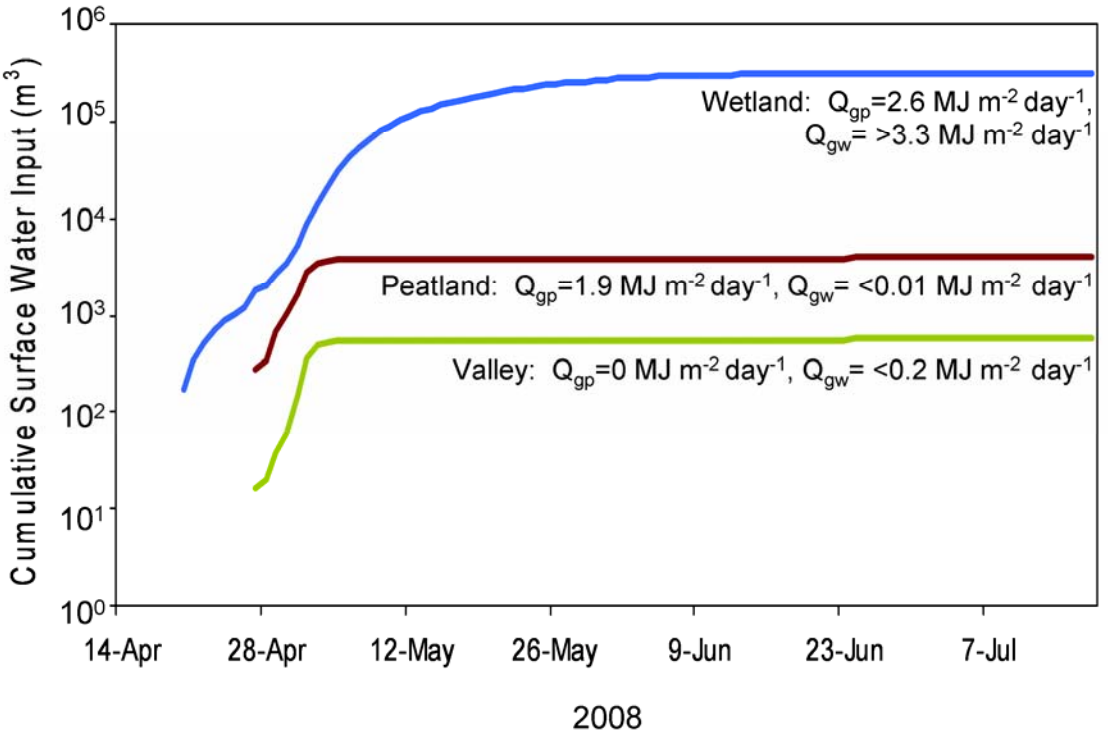

Figure 6.4: Surface water input to the sites (snowmelt runoff at all sites and additional lake input at wetland site) and potential amount of energy from water available for ground thaw at each site. Q_{gp} is conductive heat energy from ponded water and Q_{gw} is advective heat energy from surface water flow. The wetland Q_{gw} of 3.3 MJ m^{-2} day^{-1} is derived from dividing the overall site daily mean of 1.09x105 MJ day^{-1} evenly over the 3.3 ha site. However, the actual fraction of area influenced by surface water was much smaller. For example, 35% of the 3.3 ha site had flowing or standing water on 6 June, resulting in ~9.5 MJ m^{-2} day^{-1} of potential Q_{gw} available for transfer into the frozen ground. See Eq. 13 for details on energy calculations.

6.1.4 Discharge

Surface discharge from the wetland site was observed on 12 April and continued on and off even when bedrock runoff briefly terminated between 14 April and 26 April. At the wetland site, there were two outlets bisected by a bedrock island; both drained into Vital Lake. Surface discharge from the wetland site was observed throughout the study period while the peatland and valley sites had surface discharge only in the snowmelt period and from some rainfall events (e.g. 24 June) (Figure 6.3). Over the study period, ~290 mm, ~1400 mm, ~9630 mm of Q_s was

measured from the peatland, valley, and wetland site, respectively.

Subsurface outflow from the wetland amounted to 0.001 mm day^{-1} and flow out of the valley site was expected to be similar to the subsurface input (maximum 0.04 mm day^{-1}). At the peatland site, subsurface flow averaged 1.8 mm m^{-1}.

6.1.5 Evapotranspiration

The peatland had an overall daily ET rate of 2.5 mm day^{-1}, with a total loss of 208 mm over the study period (Figure 6.3a). Surface ponding at the wetland site was more widespread and was maintained longer than at the peatland site. The more extensive ponding and different vegetation cover led to more evaporative loss at the wetland site; the daily mean ET was 3.2 mm day^{-1} for a total loss of 302 mm over the study period (Figure 6.3c). The valley site was the driest of the three as well as the site with the highest surface and aerodynamic resistances. The valley lost water to the atmosphere at a daily mean rate of 2.1 mm day^{-1} and had a total loss of 153 mm (Figure 6.3b).

6.1.6 Storage Change

Change in storage as calculated with equation 1 or 18 differed across the three sites during the study. The peatland and valley sites experienced a storage deficit as outputs exceeded inputs by the end of the study. At the peatland site, there was an overall storage loss of 95 mm, while there was a storage loss of 100 mm at the valley site (Figures 6.3a and 6.3b). In contrast, the wetland site had an overall storage gain of 44 mm (Figure 6.3c) due to the large inputs of snowmelt, bedrock runoff and Lake 690 water during early spring. Although there was continuous surface inflow into the site from Lake 690, a decline in storage occurred coincident with declining Lake 690 inflow in mid-June onward. .

6.2 Ground Heat Fluxes

6.2.1 Conductive and Advective Ground Heat into the Ground

Positive values of Q_{gs} began on 30 April at the peatland site, 5 May at the valley site and 17 May at the wetland site. At the peatland site, daily Q_{gs} averaged 1.1 MJ m^{-2} day^{-1} for a sum of 83 MJ m^{-2} over the study period. The valley site had a mean daily rate of 0.5 MJ m^{-2} day^{-1} and a total of 36 MJ m^{-2} of Q_{gs} over the study period at. The daily average Q_{gs} at the wetland site was 2.0 MJ m^{-2} day^{-1}, and the total over the study period was 113 MJ m^{-2}.

The Q_{gp} was only computed for dates when there was surface ponding (see section 5.1 for detailed description of surface ponding patterns). From 9 May to 9 July, the fraction of area flooded at the peatland site dropped from 0.38 to 0.06. At the wetland site, the first recorded fraction of flooded area was also 0.38, but on 28 May and decreased to 0.22 by 8 July. The peatland had surface flow only during snowmelt. Flooded areas at the wetland site included both stagnant ponding and surface flow. It was difficult to distinguish the two categories of flooding at low flow locations so all areas with surface water were grouped into one category and thus, the energy from the flooded areas ranged from the Q_{gp} value to the Q_{gw}. The valley site experienced only a brief period of surface ponding during snowmelt so values of Q_{gp} were negligible. Flooded locations in the peatland site transferred 147 MJ m^{-2} of Q_{gp} to the soil at a mean daily rate of 1.9 MJ m^{-2} day^{-1} (Figure 6.4). At the wetland site, 158 MJ m^{-2} of energy was transferred from surface ponding at a comparable mean daily rate of 2.6 MJ m^{-2} day^{-1} (Figure 6.4).

Thermal conduction transfers heat to the thawing front, but non-conductive heat transfer (e.g. from infiltration and percolation) can also contribute large quantities of heat to the thawing front (Kane et al., 2001). Q_{gw} calculation for snowmelt runoff started on 27 April when runoff across the bedrock surface was observed. The mean values were 0.005 MJ m^{-2} day^{-1} at the

peatland site, 0.2 MJ m^{-2} day^{-1} at the valley site and 0.003 MJ m^{-2} day^{-1} at the wetland. In contrast, the Lake 690 water input during the study period carried a daily mean of $1.09x10^5$ MJ day^{-1} of Q_{gw} into the wetland site, or 3.3 MJ m^{-2} day^{-1} if this flowing water was over the entire site (Figure 6.4). Since the areal extent of flowing water was never 100% over the site, the available Q_{gw} was >3.3 MJ m^{-2} day^{-1}. Recall from above that only the fraction of the wetland with flowing water had Q_{gw} available and the available energy was concentrated to only this area. For instance, on 6 June, 35% of the 3.3 ha site was flooded and if it is considerate that all this fraction of area had flowing water, a maximum (accounting for some loss to the atmosphere) of 9.5 MJ m^{-2} day^{-1} of Q_{gw} was available for transfer into the frozen ground. Q_{gw} was also calculated for rain water, but was negligible due to the low rain temperature and input during the study period.

The hydrological processes at the three study sites led to negligible Q_{fz} influence during the snowfree part of the study period. As found in previous sections, large fractions of the peatland and wetland areas remained saturated through the study period, making Q_{fz} unimportant. While Q_{fz} could be important at unsaturated locations (e.g. valley site), only 42 mm of precipitation fell during the study period, with all events being ≤10 mm (Figure 6.1). Studies conducted at nearby sites have shown that for events ≤12 mm there is no soil moisture response at 0.30 m depth due to interception by dry lichen and moss mats (Bello and Arama, 1980; Spence and Woo, 2003). Further, reduced percolation of infiltrated water would be expected in unsaturated peat soils because of very low hydraulic conductivities (Beheim, 2006). Thus, there was only potential for infiltrating rain water to reach the thawing front in early spring when the thawing front was at or near the ground surface.

6.2.2 Modified Péclet Numbers for Northern Wetlands

When all the advective energies were applied uniformly over the study site areas, the peatland site had a mPe of 0.0004 and the valley site had a mPe of 0.09 per unit area. If the topological controls influencing the peatland and wetland sites (i.e. isolated and surrounded by bedrock) were the same at the wetland site, its mPe would have been in the same order of magnitude as at the peatland site with 0.0002. However, because of the wetland's important connection to Lake 690, the mPe at the site was serveral orders of magnitudes larger than the other two sites at 1.1.

6.3 Discussion

A combination of a reduction in lateral water input, low precipitation to evapotranspiration ratio (0.20 at the peatland site, 0.27 at the valley site and 0.13 at the wetland site) and ground thaw led to the overall drying trend in soil condition observed over the study period. However, lateral water exchanges were the cause of intra- and inter-site variability in soil moisture and ground thaw patterns described in Chapter 5. The ponded and flowing surface water were the key differences among the sites since the water largely controlled the amount of energy available for thawing. As discussed in Chapter 5, site topology was a key control on how much water was received. For example, the wetland site was a flow-through system because it was situated between two lakes (690 and Vital). The Lake 690 inflow had an important influence on the spatial distribution of soil moisture at the wetland site. The presence of aufeis resulting from Lake 690 flooding at this site led to a prolonged melt period and the lake water sustained the site wetness. This contributed to the observed increase in soil moisture heterogeneity over the study period.

The surface inflow also strongly influenced the spatial patterns of frost table depth and thaw at the wetland site. Here, the ice rich soil required a large quantity of latent ground heat to thaw it. The large amount of potential advective heat transferred into the ground from the lake water thawed soil along parts of the flow routes to depths ≥1 m before the wetland was fully snow-free. Although much of this surface inflow to the wetland site was drained to Vital Lake, the water had frequent contact with the soil as it flowed in and out of the soil toward Vital Lake. Some of this energy was lost to the atmosphere (e.g. through evapotranspiration), but due to the large heat content available, there remained ample energy for transfer into melting the frozen ground. Under a 'normal' zero-curtain situation, locations with more ice rich conditions in the winter months thaw at a slower rate than locations that are not ice rich (Carey and Woo, 1998a). However, when surface water is plenty as observed at two of the study sites, it can enhance ground thaw enough to efficiently thaw even saturated frozen soil. Other key differences between this subarctic and Carey and Woo's high arctic site may be the number of thawing degree-days. In comparison, the peatland and valley sites thawed at a slower rate than the wetland site in the spring due to the absence of advective ground heat from lake water as dictated by individual site topology. The peatland and valley sites did not have continuous surface lateral inflow. Runoff per unit area into the peatland and valley sites were only ~3% and ~14% of that received by the wetland site, respectively. The meltwater runoff did not add a significant amount of advective energy into the peatland and valley soil due to the similarity in temperature between the cool meltwater and cool soil during the freshet. However, at the peatland site, the extensive surface ponding in the hollows as controlled by the gentle topography and hummock-hollow typology kept the peat saturated for longer and increased the thermal conductivity of this organic soil. This enhanced local ground thaw, creating high spatial heterogeneity in the frost table

position. These results contrast with those of Mackay (1981) and Quinton and Marsh (1995). Their work with mineral hummocks and peaty hollows shows peat decreases downward penetration of heat which leads to less thaw in hollows (Mackay, 1981; Quinton and Marsh, 1995). The soil type and hollow ponding were some of the causes of the difference observed at the Baker Creek sites compared to the sites studied by Mackay (1981) and Quinton and Marsh (1995).

Presented thus far is a discussion of how conductive and advective heat energies regulated soil thawing along flow routes and ponded areas. However, radiative energy (Q_{gs}) was important to ground thaw at locations without surface flow or ponding. Locations only influenced by radiative energy were found to commonly have more homogeneous thaw depths and slower thaw rates. For instance, at the valley site, negligible amounts of Q_{gp} and Q_{gw} were available due to limited surface water storage. Thus, the drier site condition mostly explained the site's slower thaw rate. Differences in Q_{gs} among the sites were primarily due to higher soil thermal conductivity in the increasingly wetter soils in the peatland and wetland. Furthermore, the conifers and bedrock at the valley site decreased net radiation received at the ground surface, which further decreased the radiative energy available to the soil. Soil wetting from small rain events during the field season often only rewetted surface soils. Overall rain influence on ground heat flux was limited and this was comparable to the small amount of heat from rain water found in Resolute Bay, Nunavut and the subarctic Yukon Territory (Woo and Xia, 1996; Carey and Woo, 2000).

The wetland mPe was four orders of magnitudes higher than the peatland mPe due to more predominant external versus internal controlling processes on the energy budget. The energy from the lake water accelerated localized ground thaw rate at the wetland while the peatland

thaw rate was relatively more gradual. The advective and conductive energies at the wetland site were of approximate equal importance whereas the conductive energy at the other two sites was of more importance to the sites' energy fluxes. The valley had little surface ponding (i.e. low Qgs) and had a mPe that was two orders of magnitude larger than the peatland. The size of the valley was smaller than the other two sites and so the energy from the inflow runoff volume amounted to more energy per unit area. These important links between energy and water fluxes support the energy-based paradigm for runoff generation proposed by Quinton and Carey (2008).

CHAPTER 7:

CONCLUSIONS

Frozen ground in cold regions has unique effects on subsurface water distribution and storage. This thesis shows a diverse and dynamic spatiotemporal interaction between soil moisture and ground thaw over the subarctic landscape. Temporal patterns show that these variables are mainly responding to seasonal forcing. The temporal data presented here and the high resolution intra-site surveys contribute a great amount of insight into this very heterogeneous ground thaw process. The spatial patterns show that the two variables are feedbacks of one another (i.e. generally when soil moisture increases, ground thaw is enhanced which facilitates the transport of water). The wettest surface soils in the spring often coincide with locations of the deepest frost table depth later in the summer. These results contrast with findings from regions without frozen ground that possess a stable active soil column. In these regions locations with shallow soil tend to be the wettest. Spatiotemporal soil moisture and ground thaw patterns and correlation differ over the landscape, demonstrating that all soil filled areas cannot be treated equally in hydrologic models. A spectrum of correlations between soil moisture and ground thaw among wet to dry sites exists. The interaction between soil moisture and ground thaw is more time dependent when sites are drier. Examining the key hydrological and energy controls on the above patterns found that the relative topology, topography and typology influences at each site dictate the energy and water flux controls on shallow soil moisture and ground thaw. Overall, soil moisture, on the one hand, influences the thermal conductivity and heat energy available for ground thaw. On the other hand, deeper ground thaw increases water storage capacity. Soil moisture and frost table patterns are largely controlled by surface water. The water keeps soil moisture high and in the right conditions permits the transfer

of substantial quantities of latent heat to the ground, leading to more soil thaw than at sites lacking substantial surface ponding or flow. These energy influences can be quantified with the mPe. The mPe could be used in future studies to categorize soil filled areas and be incorporated in hydrological model parameterization. Also, a soil filled area's position in the T^3 template and its mPe can be used in combination to indicate a site's soil moisture-ground thaw patterns and interactions. For instance, a site with a mPe of 1.0 and a T^3 dominated by topology is expected to have similar areal extent, hydrological and energy controls as the wetland site examined in this study.

The results provide explanations for the shallow soil moisture-ground thaw patterns observed by linking these patterns with hydrological processes related to water budget nuances among the three sites. Using similar methods to study other cold regions (e.g. high arctic), and incorporating groundwater flow and deeper soil moisture into the calculation of mPe in future research are recommended. Such studies would complement these findings and provide a strong base for upscaling, parameterizing and incorporating the results into cold region hydrological models to predict subsurface water storage.

REFERENCES:

Allen, R.G., Jensen, M.E., Wright, J.L. and Burman, R.D.: Operational estimates of reference evapotranspiration, Agron. J., 81, 650-662, 1989.

Beheim, E.: The effect of peat land drainage and afforestation on runoff dynamics: Consequences on floods in the Glomma River, in: Environmental Role of Wetlands in Headwaters, Springer, Dordrecht, 59-76, 2006.

Bello, R. and Arama, A.: Rainfall interaction in lichen canopies, Climatol. Bull., 23, 74-78, 1980.

Black, P.B. and Miller, R.D.: Hydraulic conductivity and unfrozen water content of air-free frozen soil, Water Resour. Res., 26, 323-329, 1990.

Blyth, E.M., Finch, J., Robinson, M. and Rosier, P.: Can soil moisture be mapped onto the terrain? Hydrol. Earth Syst. Sc., 8, 923–930, 2004.

Buttle, J.M.: Mapping first-order controls on streamflow from drainage basins: The T^3 template, Hydrol. Process., 20, 3415-3422, 2006.

Carey, S.K. and Woo, M.-k.: A case study of active layer thaw and its controlling factors, in: Proceedings of the Seventh International Conference on Permafrost, Yellowknife, Canada, 23-27 June 1998, 127–132, 1998a.

Carey, S.K. and Woo, M.-k.: Snowmelt hydrology of two subarctic slopes, Southern Yukon, Canada, Nord. Hydrol., 29, 331-346, 1998b.

Carey, S.K. and Woo, M.-k.: Within-slope variability of ground heat flux, subarctic Yukon, Phys. Geogr. 21, 407-417, 2000.

Carey, S.K. and Woo, M.-k.: Slope runoff processes and flow generation in a subarctic, subalpine catchment. J. Hydrol., 253, 110-119, 2001.

Carlson, T.: Modeling stomatal resistance: an overview of the 1989 workshop at the Pennsylvania State University, Agr. Forest Meteorol., 54, 103-106, 1991.

Dalton, J.: Experimental essays on the constitution of mixed gases: on the force of steam or vapour from water or other liquids in different temperatures, both in a Torricelli vacuum and in air; on evaporation; and on expansion of gases by heat, Manchester Lit. Phil. Soc. Mem., 5, 536-602, 1802.

Devito, K.J., Hill, A.R. and Roulet, N.: Groundwater-surface water interactions in headwater forested wetlands of the Canadian Shield, J. Hydrol., 181, 127-147, 1996.

de Vries, D.A.: Thermal properties of soils, in: Physics of Plant Environment, North-Holland Publishing Co., Amsterdam, 210-235, 1963.

Dingman S.L.: Hydrology of Glenn Creek watershed, Tanana basin, Central Alaska, U.S. Army CRREL, Hanover, NH, Res. Rep. 297, 115 pp., 1971.

Dingman, S.L.: Hydrologic effects of frozen ground: literature review and synthesis, Special Report 218, U.S. Army Cold Regions Research and Engineering Laboratory, Hanover, NH, 59 pp., 1975.

Dingman, S.L.: Physical Hydrology, 2, Waveland Press, Long Grove, 646 pp., 2008.

England, C.B. and Holtan, H.N.: Geomorphic grouping of soils in watershed engineering. J. Hydrol., 7, 217-225, 1969.

Faria, D.A., Pomeroy, J.W. and Essery, R.L.H.: Effect of covariance between ablation and snow water equivalent on depletion of snow-covered area in a forest, Hydrol. Process., 14, 2683-2695, 2000.

Farouki, O.T.: Thermal properties of soils, CRREL Monograph No. 81-1, U.S. Army Cold Regions Research and Engineering Laboratory, Hanover, NH, 136 pp., 1981.

Granger, R.J., Gray, D.M. and Dyck, G.E.: Snowmelt infiltration to frozen prairie soils, Can. J. Earth Sci., 21, 669-677, 1984.

Gray, J.T., Pilon, J. and Poitevin, J.: A method to estimate active-layer thickness on the basis of correlations between terrain and climatic parameters as measured in northern Quebec, Can. Geotech. J., 25, 607-616, 1988.

Grayson, R.B., Blöschl, G., Western, A.W. and McMahon, T.A.: Advances in the use of observed spatial patterns of catchment hydrological response, Adv. Water Resour., 25, 1313-1334, 2002.

Grayson, R.B., Western, A.W., Chiew, F.H.S. and Blöschl, G.: Preferred states in spatial soil moisture patterns: Local and nonlocal controls, Water Resour. Res., 33, 2897-2908, 1997.

Gustard, A.: Analysis of river regimes, in: The Rivers Handbook, 1, Blackwell Scientific, Oxford, 29-47, 1992.

Hastings, S.J., Luchessa, S.A., Oechel, W.C. and Tenhunen, J.D.: Standing biomass and foothills of the Phillip Smith Mountains, Alaska. Holarctic Ecol., 12, 304-311, 1989.

Hayashi, M., Goeller, N., Quinton, W.L. and Wright, N.: A simple heat-conduction method for simulating the frost-table depth in hydrological models, Hydrol.. Process., 21, 2610–2622, 2007.

Heron, R. and Woo, M.-k.: Snowmelt computation for a High Arctic site, in: Proceedings of the 35th Eastern Snow Conference, Hanover, New Hampshire, 162-172, 1978.

Hinkel, K.M. and Nelson, F.E.: Spatial and temporal patterns of active layer thickness at Circumpolar Active layer Monitoring (CALM) sites in northern Alaska, 1995-2000, J. Geophys. Res., 108, doi: 10.1029/2001JD000927, 2003.

Hinzman, L.D., Kane, D.L. and Everett, K.R.: Hillslope hydrology in an Arctic setting, in: Proceedings of the Sixth International Conference on Permafrost, Beijing, China, 5-9 July 1993, 257-271, 1993.

Hodgson, R. and Young, K.L.: Preferential groundwater flow through a sorted net landscape, arctic Canada, Earth Surf. Proc. Land., 26 319-328, 2001.

Hopkinson, C. and Fox, A.: IP3 LiDAR collaborative research data report, Applied Geomatics Research Group, Centre of Geographic Sciences, Nova Scotia, 21 pp., 2008.

James, A.L. and Roulet, N.T.: Investigating hydrologic connectivity and its association with threshold change in runoff response in a temperate forested watershed, Hydrol. Process., 21, 3391-3408, 2007.

Jarvis, P.G.: The interpretation of the variations in leaf water potential and stomatal conductance found in canopies in the field, Philos. T. Roy. Soc. B, 273, 593–610, 1976.

Johnson, D., Kershaw, L.J., MacKinnon, A., and Pojar, J: Plants of the Western Boreal Forest and Aspen Parkland, Lone Pine, Edmonton, 1995.

Kane, D.L., Hinkel, K.M., Goering, D.J., Hinzman, L.D. and Outcalt, S.I.: Non-conductive heat transfer associated with frozen soils, Global Planet. Change, 29, 275-292, 2001.

Körner, C.: Leaf diffusive conductances in the major vegetation types of the globe, in: Ecophysiology of Photosynthesis, Springer-Verlag, New York, 463-490, 1994.

Lafleur, P.M.: Leaf conductance of four species growing in a subarctic marsh, Can. J. Botany, 66, 1367-1375, 1988.

Lafleur, P.M. and Schreader, C.P.: Water loss from the floor of a subarctic forest, Arctic Alpine Res., 26, 152-158, 1994.

Landals, A.L. and Gill, D.: Differences in volume of surface runoff during the snowmelt period: Yellowknife, Northwest Territories, in: Proceedings of the International Symposia on the Role of Snow and Ice in Hydrology, IAHS, Banff, September 1972, 107, 927-942, 1972.

Larson, D.W. and Kershaw, K.A.: Studies of lichen-dominated systems. XVIII. Morphological control of evaporation in lichens. Can. J. Botany, 54, 2061-2073, 1976.

Luthin, J.N.: Drainage Engineering, Wiley, New York, 1966.

Lyon, S.W. and Troch, P.A.: Hillslope subsurface flow similarity: Real-world tests of the hillslope Péclet number, Water Resour. Res., 43, W07450, doi:10.1029/2006WR005323, 2007.

Mackay, J.R.: Active layer slope movement in a continuous permafrost environment, Garry Island, Northwest Territories, Canada, Can. J. Earth Sci., 18, 1666-1680, 1981.

Nicholson, F.H.: Permafrost Distribution and Characteristics near Schefferville, Quebec, in: Proceedings of the Third International Permafrost Conference, Edmonton, AB, 10-13 July 1978, 427-433, 1978.

Outcalt, S.I., Nelson, F.E. and Hinkel, K.M.: The zero-curtain effect: heat and mass transfer across an isothermal region in freezing soil, Water Resour. Res., 26, 1509-1516, 1990.

Park, J.O.: Vegetation patterns and moisture availability in the Baker Creek Basin, near Yellowknife, NWT, M.Sc. Thesis, University of Alberta, Edmonton, 1979.

Penman, H.L.: Natural evaporation from open water, bare soil, and grass, P. R. Soc. Lond. A Mat., 193, 120-145, 1948.

Pennock, D.J.: Multi-site assessment of cultivation-induced soil change using revised landform segmentation procedures, Can. J. Soil Sci., 83, 565-580, 2003.

Pennock, D.J., Zebarth, B.J. and de Jong, E.: Landform classification and soil distribution in hummocky terrain, Saskatchewan, Canada, Geoderma, 40, 297-315, 1987.

Perron, J.T., Dietrich, W.E. and Kirchner, J.W.: Controls on the spacing of first-order valleys, J. Geophys. Res., 113, F04016, doi:10.1029/2007JF000977, 2008.

Pomeroy, J.W. and Gray, D.M.: Snow Accumulation, Relocation and Management, National Hydrology Research Institute Science Report No. 7, Environment Canada: Saskatoon, 144 pp, 1995.

Pomeroy, J.W., Marks, D., Link, T., Ellis, C., Hardy, J., Rowlands, A. and Granger R.: The impact of coniferous forest temperature on incoming longwave radiation to melting snow, Hydrol. Process., DOI: 10.1002/hyp.7325, 2009.

Quinton, W.L. and Carey, S.K.: Towards an energy-based runoff generation theory for tundra landscapes, Hydrol. Process., 22, 4649-4653, 2008.

Quinton, W.L., Gray, D.M., and Marsh, P.: Subsurface drainage from hummock-covered hillslopes in the arctic-tundra, J. Hydrol., 237, 113–125, 2000.

Quinton, W.L., Hayashi, M., and Pietroniro, A.: Connectivity and storage functions of channel fens and flat bogs in northern basins, Hydrol. Process., 17, 3665-3684, 2003.

Quinton, W.L. and Marsh, P.: Subsurface runoff from tundra hillslopes in the continuous permafrost zone, in: Report and Proceedings of the International GEWEX Workshop on Cold-Season/Region Hydrometeorology, Banff, AB, 22-26 May 1995, 51-55, 1995.

Quinton, W.L. and Marsh, P.: The influence of mineral earth hummocks on subsurface drainage in the continuous permafrost zone, Permafrost Periglac., 9, 213-228, 1998.

Quinton, W.L. and Marsh, P.: A conceptual framework for runoff generation in a permafrost environment, Hydrol. Process., 12, 2563-2591, 1999.

Rodriguez-Iturbe, I., D'Odorico, P., Laio, F., Ridolfi, L. and Tamea, S.: Challenges in humid land ecohydrology: Interactions of water table and unsaturated zone with climate, soil, and vegetation, Water Resour. Res., 43, W09301, doi:10.1029/2007WR006073, 2007.

Rouse, W. R., Carlson, D.W. and Werck, E. J.: Impacts of summer warming on the energy and water balance of wetland tundra, Climatic Change, 22, 305-326, 1992.

Shirazi, T., Allen, D.M., Quinton, W.L. and Pomeroy, J.W.: Estimating soil thaw energy in sub-Alpine tundra at the hillslope scale, Wolf Creek, Yukon Territory, Canada, Hydrol. Res., 40, 1-18, 2009.

Shuttleworth, W.J.: Evaporation, in: Handbook of Hydrology, McGraw-Hill, New York, 4.1-4.53, 1993.

Sinai, G., Zaslavsky, D. and Golany, P.: The effect of soil surface curvature on moisture and yield - Beer Sheba observation, Soil Sci., 132, 367-375, 1981.

Spence, C.: The effect of storage on runoff from a headwater subarctic shield basin, Arctic, 53, 237-247, 2000.

Spence, C.: Hydrological processes and streamflow in a lake dominated watercourse, Hydrol. Process., 20, 3665-3681, 2006.

Spence C., Guan, X.J., Phillips, R., Hedstrom, N., Granger, R. and Reid, B.: Storage dynamics and streamflow in a catchment with a variable contributing area, Hydrol. Process., doi: 10.1002/hyp.7492, 2009.

Spence, C. and Rouse, W.R.: The energy budget of Canadian Shield subarctic terrain and its impact on hillslope hydrological processes, J. Hydrometeorol., 3, 208-218, 2002.

Spence, C. and Woo, M.-k.: Hydrology of subarctic Canadian Shield: bedrock upland, J. Hydrol., 262, 111-127, 2002.

Spence, C. and Woo, M.-k.: Hydrology of subarctic Canadian shield: soil-filled valleys, J. Hydrol., 279, 151-166, 2003.

Spence, C. and Woo, M.-k.: Hydrology of subarctic Canadian Shield: heterogeneous headwater basins, J. Hydrol., 317, 138-154, 2006.

Stüwe, K.: Geodynamics of the Lithosphere, 2, Springer, Heidelberg, 2007.

Spence, C.: The effect of storage on runoff from a headwater subarctic shield basin, Arctic, 53, 237-247, 2000.

Tromp van Meerveld, I. and McDonnell, J.J.: Comment to "Spatial correlation of soil moisture in small catchments and its relationship to dominant spatial hydrological processes, Journal of Hydrology 286: 113-134", J. Hydrol., 303, 307-312, 2005.

Tromp-van Meerveld, H.J. and McDonnell, J.J.: Threshold relations in subsurface stormflow 2. The fill and spill hypothesis, Water Resour. Res., 42, W02411, doi:10.1029/2004WR003800, 2006.

Verseghy D.L., McFarlane, N.A. and Lazare, M., A Canadian land surface scheme for GCMs, II. Vegetation model and coupled runs, Int. J. Climatol., 13, 347–370, 1993.

Wight, J.B.: Aspects of evaporation and evapotranspiration in the water balance of Baker Creek Basin, near Yellowknife, NWT, M.Sc. Thesis, University of Alberta, Edmonton, 1973.

Western, A.W., Blöschl, G. and Grayson, R.B.: Toward capturing hydrologically significant connectivity in spatial patterns, Wat. Resour. Res., 37, 83-97, 2001.

Western, A.W., Grayson, R.B. and Blöschl, G.: Scaling of soil moisture: A hydrologic perspective. Annu. Rev. Earth Pl. Sc., 30, 149-180, 2002.

Western, A.W., Zhou, S.L., Grayson, R.B., McMahon, T.A., Blöschl, G. and Wilson, D.J.: Spatial correlation of soil moisture in small catchments and its relationship to dominant spatial hydrological processes, J. Hydrol., 286, 113-134, 2004.

Wolfe, S.A.: Living with Frozen Ground: A Field Guide to Permafrost in Yellowknife, Miscellaneous Report 64, Geological Survey of Canada, Northwest Territories, 71 pp., 1998.

Woo, M.-k.: A guide for ground based measurement of arctic snow cover, Canadian Snow Data CD, Meteorological Service of Canada, Downsview, Ontario, 30 pp., 1997.

Woo, M-k and DiCenzo, P.D.: Hydrology of small tributary streams in a subarctic wetland, Can. J. Earth Sci., 26, 1557–1556, 1989.

Woo, M.-k. and Marsh, P.: Response of soil moisture change to hydrological processes in a continuous permafrost environment. Nord. Hydrol., 21, 235-252, 1990.

Woo, M.-k. and Steer, P.: Slope hydrology as influenced by thawing of the active layer, Resolute, N. W.T., Can. J. Earth Sci., 20, 978-986, 1983.

Woo, M.-k. and Winter, T.C.: The role of permafrost and seasonal frost in the hydrology of northern wetlands in North America, J. Hydrol., 141, 5-31, 1993.

Woo, M.-k. and Xia, Z.: Effects of hydrology on the thermal conditions of the active layer, Nord. Hydrol., 27, 129-142, 1996.

Wright, N., Hayashi, M. and Quinton, W.L.: Spatial and temporal variations in active layer thawing and their implication on runoff generation in peat-covered permafrost terrain, Wat. Resour. Res. 45, W05414, doi:10.1029/2008WR006880, 2009.

Zebarth, B.J. and De Jong, E.: Water-flow in a hummocky landscape in Central Saskatchewan, Canada .I. Distribution of water and soil, J. Hydrol., 107, 309-327, 1989.

APPENDIX A:

TDR CALIBRATION CURVES

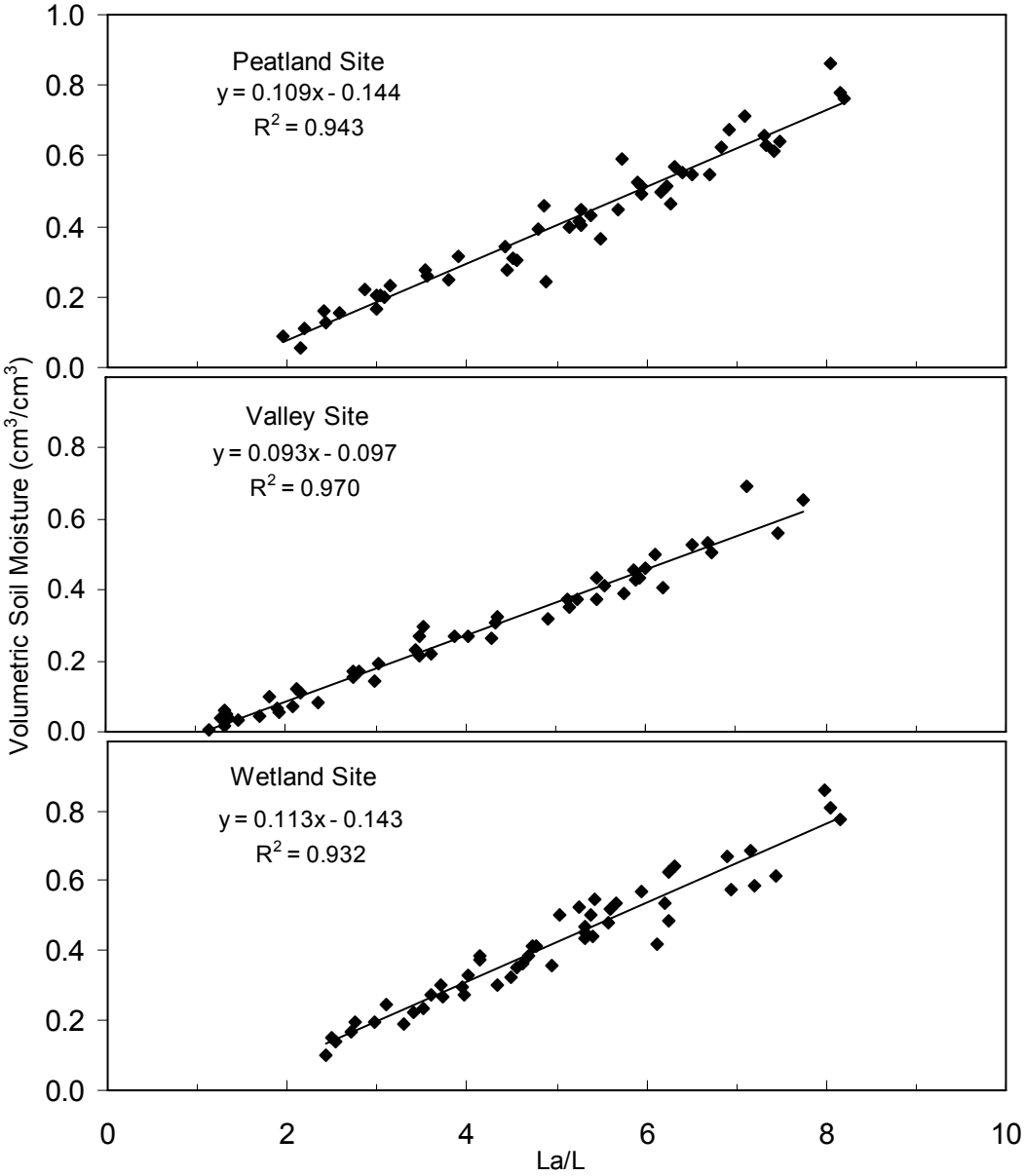

Figure A.1: Laboratory time domain reflectometry calibration curves from site specific soil samples. La/L is the square root of the dielectric constant.

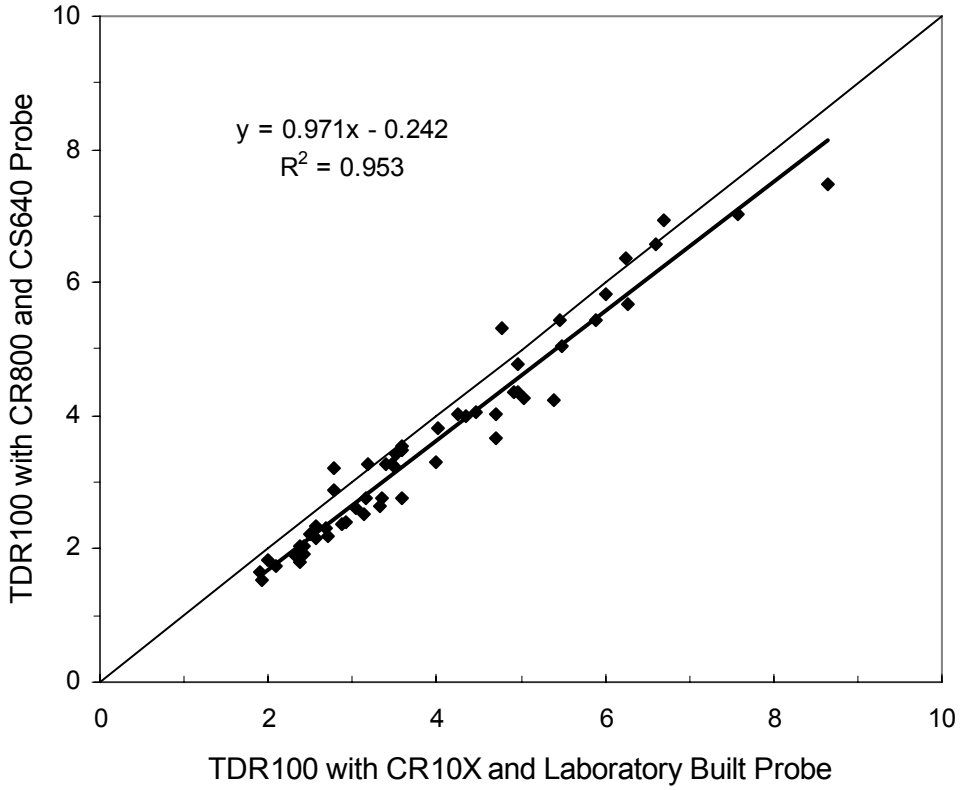

Figure A.2: Standardizing the CR10X unit against the CR800 unit by measuring the same soil samples with both units. The thin diagonal line represents the 1:1 ratio and the thick line represents the line of best fit.

APPENDIX B:

LAKE 690 STAGE-DISCHARGE CURVES

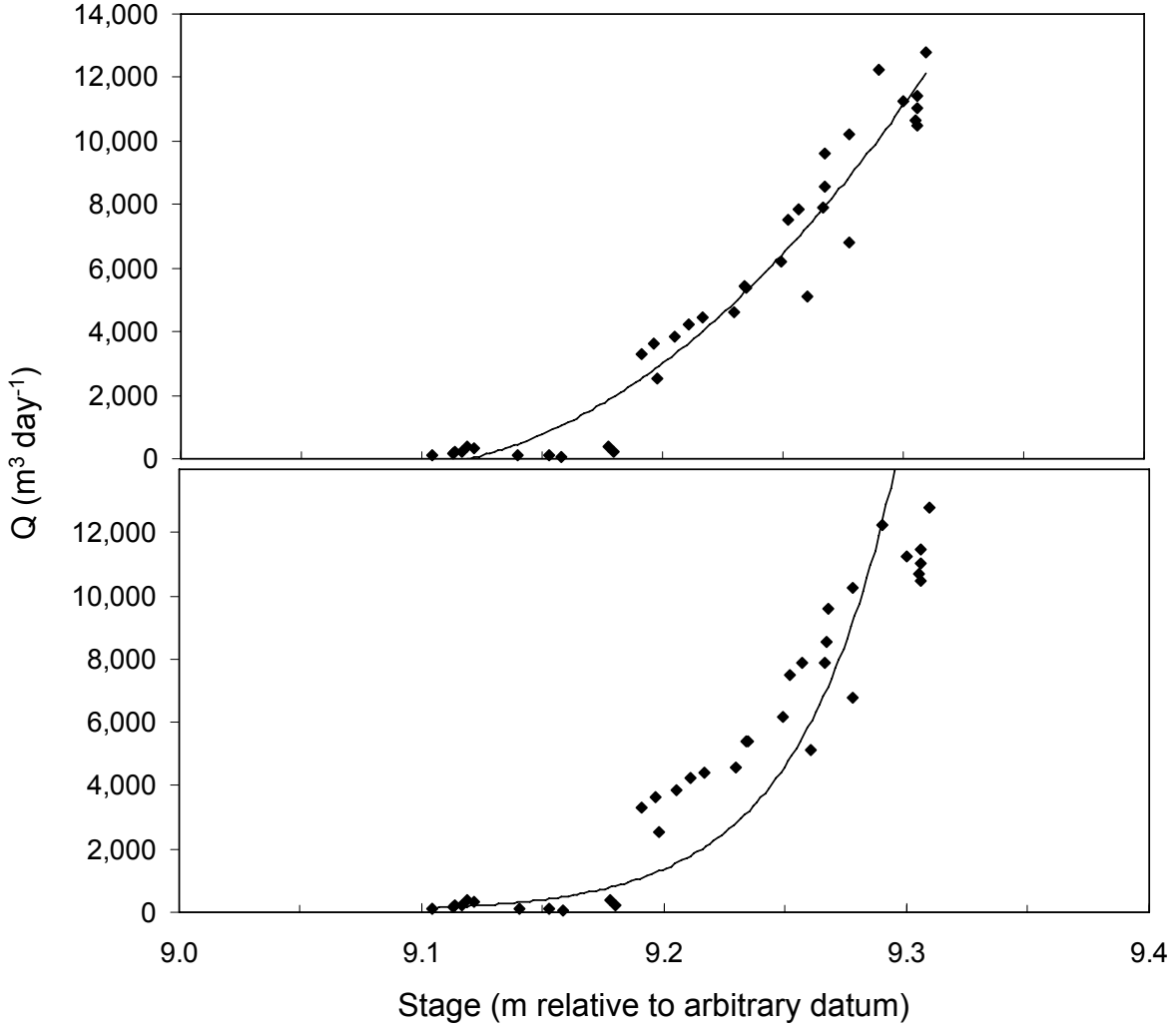

Figure B.1: Lake 690 outlet stream discharge (Q) rating curves for stage ≥9.17 m (relative to arbitrary datum) with an r^2 value of 0.95 ($Q= 243695.6stage^2 - 4427169.2stage + 20106563.7$, top graph), and stage <9.17 with an r^2 value of 0.82 ($Q=2x10^{-95}e^{24.5stage}$, bottom graph).